Quaternary Science Reviews 41 (2012) 1–21

Contents lists available at SciVerse ScienceDirect

Quaternary Science Reviews

journal homepage: www.elsevier.com/locate/quascirev

Invited review

Deglacial changes of the southern margin of the southern westerly winds revealed by terrestrial records from SW Patagonia (52°S)

P.I. Moreno [a,*], R. Villa-Martínez [b], M.L. Cárdenas [c], E.A. Sagredo [d]

[a] Department of Ecological Sciences and Institute of Ecology and Biodiversity, University of Chile, Las Palmeras 3425, Ñuñoa, Santiago, Chile
[b] Centro de Estudios del Cuaternario (CEQUA), Avenida Bulnes 01890, Casilla 737, Punta Arenas, Chile
[c] Department of Earth and Environmental Sciences, CEPSAR, The Open University, Walton Hall, Milton Keynes MK7 6AA, UK
[d] Department of Geology, University of Cincinnati, Cincinnati, OH 45221, USA

ARTICLE INFO

Article history:
Received 8 September 2011
Received in revised form
26 January 2012
Accepted 2 February 2012
Available online xxx

Keywords:
Southwest Patagonia
Southern Westerly Winds
Last glacial termination
Atmospheric CO_2 variations

ABSTRACT

Much of the ongoing discussion regarding synchrony or bipolar asynchrony of paleoclimate events has centered on the timing and structure of the last glacial termination in the southern mid- latitudes, in particular the southwestern Patagonian region (50°–55°S). Its location adjacent to the Drake Passage and near the southern margin of the southern westerly winds (SWW) allows examining the postulated links between the Southern Ocean–SWW coupled system and atmospheric CO_2 variations through the last glacial termination. Results from two sites located in the Última Esperanza area (52°S) allow us to infer SWW-driven changes in hydrologic balance during this critical time interval. These findings indicate peatland development under temperate/wet conditions between 14,600 and 14,900 cal yr BP, followed by cooling and a lake transgressive phase that led to a shallow lake during the early part of the Antarctic Cold Reversal (ACR, 13,600–14,600 cal yr BP), followed in turn by a deeper lake and modest warming during Younger Dryas time (YD, ~11,800–13,000 cal yr BP), superseded by terrestrialization and forest expansion at the beginning of the Holocene. We propose that the SWW (i) strengthened and shifted northward during ACR time causing a precipitation rise in northwestern and southwestern Patagonia coeval with mid- and high-latitude cooling and a halt in the deglacial atmospheric CO_2 rise; (ii) shifted southward during YD time causing a precipitation decline/increase in NW/SW Patagonia, respectively, high-latitude warming, and invigorated CO_2 release from the Southern Ocean; (iii) became weaker between ~10,000 and 11,500 cal yr BP causing a precipitation decline throughout Patagonia, concurrent with peak mid- and high-latitude temperatures and atmospheric CO_2 concentrations.

1. Introduction

Much discussion has generated the timing and structure of climate changes during the last glacial termination (11,000–18,000 cal yr BP) in the middle latitudes of the Southern Hemisphere. This has resulted from divergent chronologies, the complexity of millennial-scale changes during this highly variable climatic transition, differences on the interpretation and implications of paleoclimate proxies at regional and hemispheric scale and, oftentimes, on a lack of appreciation on the variable relationship between meso- and macro-scale climatic controls along geographic and temporal domains. Southwestern Patagonia and Tierra del Fuego (50°–55°S) are key regions in this discussion because they constitute the southernmost continental landmasses in the Southern Hemisphere, thus offering the potential to examine the causes and consequences of paleoclimate change on terrestrial environments located in the subantarctic zone, and the postulated links between the Southern Westerly Winds (SWW) and the Southern Ocean (SO) coupled system. Numerical modeling and stratigraphic studies over the last decades have emphasized the central role of the SWW–SO coupled system as a key component of the global climate system through its influence on productivity changes in the SO, global deep water circulation, and ocean to atmosphere heat and gas fluxes (including greenhouse gases) (Imbrie et al., 1992; Toggweiler and Samuels, 1995; Russell et al., 2006; Anderson et al., 2009; Toggweiler, 2009; Moreno et al., 2010).

Recent studies have proposed that latitudinal shifts and intensity variations of the SWW played a fundamental role in driving global and hemispheric-scale climate changes during and since the last glacial maximum (LGM) (Toggweiler et al., 2006; Anderson et al., 2009; Denton et al., 2010; Moreno et al., 2010). These findings, however, are based on limited empirical evidence and

* Corresponding author.
E-mail addresses: pimoreno@uchile.cl, pimoreno@vtr.net (P.I. Moreno).

0277-3791/$ – see front matter © 2012 Elsevier Ltd. All rights reserved.
doi:10.1016/j.quascirev.2012.02.002

additional studies are required to test the postulated structure of changes and their geographic representativeness. The behavior of the SWW during the LGM has been a particularly controversial subject in the literature for more than 20 years (Markgraf, 1989; Heusser, 1989b). Recently, Rojas et al. (2009) analyzed five coupled Global Circulation Models (GCM) conducted in the context of the Palaeoclimate Modeling Intercomparison Project Phase 2 (PMIP2), and concluded that the SWW were weaker and less zonally symmetric during the LGM simulation (21,000 cal yr BP). Several climate diagnostics pointed to a remarkable climate boundary north and south of the modern zone of maximum wind speeds at 45–50°S in southern South America, and enhanced north–south and east–west climate contrasts in precipitation derived from the SWW. Few terrestrial paleoclimate records in this vast region, however, span the critical time interval to test these GCM outputs.

When and how the SWW transitioned into the Holocene is also an elusive subject in the paleoclimate literature from the southern mid-latitudes. It is yet unclear whether this occurred in a gradual, unidirectional manner or through multiple steps including latitudinal shifts, intensity variations and reversals. Studies carried out in Torres del Paine, Estrecho de Magallanes, and Tierra del Fuego (50–55°S) (Fig. 1) indicate glacial recession from the final LGM limit and a species-depauperate colonization phase of the vegetation during the early stages of deglaciation, followed by grassland expansion, establishment of heathlands, and then woodland encroachment at the beginning of the Holocene (see Markgraf and Huber, 2011 for a recent review). The majority of the paleovegetation/paleoclimate studies have interpreted cold and dry conditions during the last glacial termination with fluctuations in effective precipitation; whether these changes were forced by temperature and/or precipitation fluctuations has not been settled in the literature. Most of those studies are based on fossil pollen records from bogs, supplemented in some cases by microscopic or macroscopic charcoal records and analysis of plant macrofossil preserved in the same core. The range of climatic interpretations based on palynological changes toward the end of the last glacial termination from sites located between 50° and 55°S include shifts toward: (i) drier conditions with intense fire activity (Puerto Harberton bog ~54°S) (Markgraf, 1993b), (ii) wetter conditions (Puerto del Hambre site) (Heusser et al., 2000), (iii) drier climate (Puerto del Hambre and Estancia Esmeralda sites, ~53°30′S) (McCulloch and Davies, 2001), (iv) drier and warmer conditions (Lago Potrok Aike, ~51°30′S) (Haberzettl et al., 2007), (v) cooler and wetter than present climate (Vega Ñandú [~51°S]) (Villa-Martínez and Moreno, 2007), and (vi) an alternating series of centennial-scale variations in temperature and precipitation (Puerto Harberton bog) (Markgraf, 1993b). Attempts to deconvolute the temperature and precipitation signals include a stable isotope record from the Puerto Harberton bog (Markgraf and Huber, 2011), interpreted as

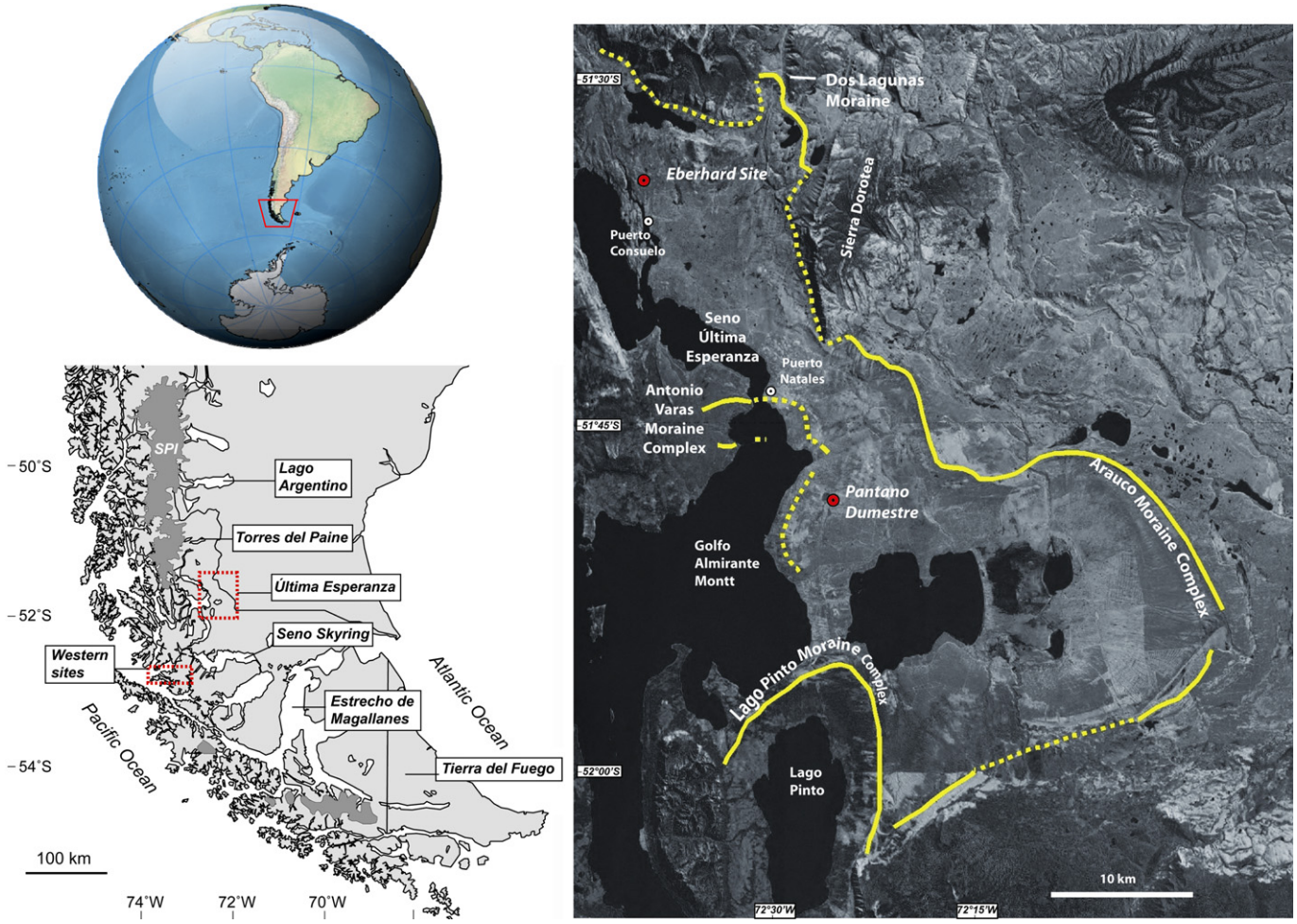

Fig. 1. Sketch map of the study region showing the location of Pantano Dumestre and Lago Eberhard, along with adjacent sectors mentioned in the text. The solid yellow lines represent ice margin positions of the Última Esperanza ice lobe during the final LGM advance, a estabilization phase, and subsequent readvance. The dashed yellow lines represent inferred ice margin positions. SPI = South Patagonian Icefield.

a paleotemperature sensor, and lake level fluctuations in Laguna Potrok Aike (Anselmetti et al., 2009), interpreted as a proxy for SWW intensity. The accuracy and geographic applicability of the latter, however, awaits replication and validation with additional sites in the region using the same proxies. The broad, often contradictory, range of interpretations highlights the need for additional detailed records and chronologies to elucidate the behavior of the southern margin of the SWW during the last glacial termination, and development of a better understanding of the spatial heterogeneities of the current and paleo landscapes.

In this study we examine the timing and structure of past changes in vegetation, fire, and depositional environments through the last glacial termination in two sites located in a formerly glaciated region of Última Esperanza (~51°45′S, 72°30′W), southwestern Patagonia, Chile. These data allow reconstruction of deglacial changes in the position and strength of the SWW and assessment of their possible role as a driver of atmospheric CO_2 variations through ventilation of CO_2-rich deep waters in the Southern Ocean.

1.1. Study area

Southwestern Patagonia and adjacent Tierra del Fuego (50–55°S) (Fig. 1) are important regions for monitoring the response of mid-latitude glaciers and land biota to the climate swings that have taken place since the LGM, and for exploring the interplay between mid and high-latitude climate change. This region of South America has been covered repeated times by Andean glaciers that expanded, coalesced, and formed the Patagonian Ice Sheet throughout the Quaternary. The Patagonian Ice Sheet extended along 1700 km over the Andes (38°–55°S), intersecting the SWW belt in its entirety. This large ice mass had a profound impact on the landscape, eroding the Andes Cordillera, depositing abundant glacial and fluvioglacial material in the adjacent lowlands, promoting the formation of proglacial lakes, changing the continental divide, and enhancing the eastward rainshadow effect of the Andes Cordillera during the LGM (Rojas et al., 2009). All these aspects had a direct impact on the land biota causing geographic shifts, displacements, fragmentation, and isolation through the establishment of climatic or physical barriers to dispersal.

This study focuses on the Última Esperanza area of southwestern Patagonia (51°30′–52°15′S, 72°–72°45′S), Chile, located on the lee side of the Andes and ~50 km SE of the South Patagonian Ice Field (Fig. 1). In this sector, the Andes Cordillera reaches its lowest elevations in the South American continent, with isolated peaks having maximum elevations of ~1500 m.a.s.l., deeply dissected by glacial valleys, channels, and fjords. The modern drainage from the Torres del Paine and Última Esperanza regions reach Golfo Almirante Montt, a gulf adjacent to Seno (=Sound) Última Esperanza area, both of which are connected to the Pacific Ocean through Paso Kirke (52°05′S, 73°05′W), a narrow (~500 m wide) and relatively shallow (65 m deep) gorge located south of Cordillera Riesco.

Outlet glaciers from the Patagonian Ice Sheet coalesced and formed the Última Esperanza piedmont lobe during the LGM, which flowed eastward out of the channels, fjords, and mountain ranges toward the extra-Andean plains in Argentinean territory. A recent study indicates at least two major LGM advances between ~17,500 and 40,000 cal yr BP, the most recent of which is marked by the Arauco Moraine Complex and the Dos Lagunas moraines in the Puerto Natales region (Sagredo et al., 2011) (Fig. 1). This was followed by glacial recession, thinning, and development of an ice-dammed proglacial lake, the Puerto Consuelo glacial lake (Sagredo et al., 2011). This lake developed when expanded Andean glaciers blocked Paso Kirke during the LGM and the last glacial termination. As a consequence, the subcontinental-scale drainage of meltwater coming from the Patagonian Ice Sheet was routed toward the Atlantic Ocean during the LGM. Subsequent glacial recession led to a transitional phase between an Atlantic- to Pacific-dominated drainage of glacial meltwater and the development of ice-dammed proglacial lakes during the last glacial termination. Variations in the surface profile and extent of the Última Esperanza and its tributary ice lobes, as well as differential isostatic rebound, controlled the elevation of the Puerto Consuelo glacial lake in response to the opening/closing of perched spillways through an intricate network of glacial valleys, channels and fjords. In the Última Esperanza area the proglacial lake attained elevations between 125 and 150 m.a.s.l. following the abandonment of the Arauco moraines and the end of a stillstand in the deglaciation process. The chronology for the highest lake level is bracketed between ~16,200 and 16,900 cal yr BP, and was followed by a regressive phase once the Última Esperanza ice lobe abandoned this stabilized position (Sagredo et al., 2011), exposing sectors with elevations below 125 m.a.s.l.

1.2. Modern climate and vegetation

The climate of Patagonia is governed by SWW, which deliver abundant precipitation to sustain glaciers, icefields, and a suite of plant communities along and across the Andes. The core of the SWW intersects the South American continent between latitudes 48 and 50°S, manifested locally as strong winds and abundant precipitation. The amount of precipitation throughout western Patagonia is strongly and positively correlated with near-surface zonal wind speeds (Garreaud, 2007). The strength of this correlation varies with latitude, season, and distance from the Pacific coast; the latter effect is induced by the topographic influence of the Andes, which constitutes a formidable barrier to low-level and tropospheric circulation in the South American continent (Moy et al., 2008). The uplift of moist air masses over the cordillera induces significant amounts of orographic precipitation on the western sectors, while subsidence farther to the east produces an overall drying effect in Argentine Patagonia toward the Atlantic. As a consequence, the correlation between zonal wind speeds and local precipitation diminishes to zero east of the Andes and then turns negative with increasing distance east of the Andes (Garreaud, 2007), implying that precipitation sources different from the SWW affect the extra-Andean region of Central Patagonia and the Atlantic seaboard.

Orographic precipitation on the windward side of the Andes increases with altitude and overall SWW strength to produce extreme environmental and climatic gradients, e.g. the annual precipitation (Dirección Meteorológica de Chile) at sea level on the Pacific coast (Isla Guarello, 50°23′S, 75°21′W) reaches 9000 mm, while precipitation declines abruptly to 200 mm in the Lago Argentino weather station (50°20′S, 72°15′W), 230 km east on the eastern Andean slopes. The climate of the Última Esperanza area is transitional between the hyperhumid oceanic climates on the western coast and the semiarid, strongly continental climates east of the Andes. Meteorological records from the Puerto Natales station (51°44′S, 72°29′W) show mean annual temperature between 6 and 7 °C with an annual range of 9–10 °C; mean annual precipitation is 513 mm and occurs evenly throughout the year with slight maxima in the months of March, April, August, and November.

The composition and distribution of the native vegetation reflects the topographically induced climatic gradients at regional scale, forming distinct vegetation zones along altitudinal and

latitudinal transects. Disturbance regimes and edaphic conditions exert important influences at smaller spatial and shorter temporal scales, subordinated to the climatically controlled vegetation zonation. Studies of the regional vegetation have led to the recognition of the Magellanic Moorland, Magellanic evergreen forest, Magellanic deciduous forest, and Patagonian steppe, along a west to east decline in precipitation from the Pacific coast to the extra-Andean region of southern Patagonia. Precipitation is a limiting factor for the eastward penetration of forests, leading to the establishment of a distinct forest-steppe ecotone east of the Andes (Villa-Martínez and Moreno, 2007; Moreno et al., 2009a). A similar boundary develops with increasing altitude, where evergreen forests give way to deciduous forests at mid elevations, extending up to the treeline. In this case, however, the limiting factor for vegetation growth is the ability to withstand low temperatures and prolonged snow cover (Lara et al., 2001). Above the treeline dominates the Andean Desert, a sparsely vegetated subnival alpine community. Here follows a brief description of the main vegetation units present in the Chilean sector of southwestern Patagonia, based primarily on Roig et al. (1985):

1) Magellanic Evergreen Forest. This is a diverse forest community that occurs mainly in the archipelagic sectors of central and southern Patagonia where annual precipitation ranges between 2000 and 6000 mm. It is dominated by *Nothofagus betuloides* (Nothofagaceae), along with the conifer *Pilgerodendron uviferum* (Cupressaceae) and other trees such as *Raukaua laetevirens* (Araliaceae), *Drimys winteri* (Winteraceae), and *Tepualia stipularis* (Myrtaceae). The shrubs *Desfontainia fulgens* (Desfontainiaceae) and *Embothrium coccineum* (Proteaceae) commonly occur near the forest edges. The shrub stratum in the forest interior is dominated by *Berberis ilicifolia* (Berberidaceae), *Escallonia serrata* (Escalloniaceae), *Lebetanthus myrsinites* (Epacridaceae), *Phylesia magellanica* (Phylesiaceae), *Luzuriaga marginata* (Luzuriagaceae), and *Chilliotrichum diffusum* (Asteraceae). Ferns are important components of this communities, occurring in the forest ground or as epiphytes on the tree trunks, dominant taxa are *Blechnum penna-marina* (Blechnaceae), *Gleichenia quadripartite* (Gleicheniaceae), *Asplenium dareoides* (Aspleniaceae), *Hymenophyllum* spp. (Hymenophyllaceae) and *Grammitis magellanica* (Grammitidaceae).
2) Magellanic Deciduous Forest. This unit corresponds to a low density forest dominated almost exclusively by the winter-deciduous *Nothofagus pumilio* and *Nothofagus antarctica* (Nothofagaceae) and occurs between 50 and 900 m.a.s.l. where the annual precipitation is 750 mm. In humid sectors (~850 mm/yr), *N. pumilio* forms mixed forests with the evergreen tree *N. betuloides*. The species-poor shrub stratum develops only near the forest edges; dominant taxa are *B. ilicifolia* (Berberidaceae), *Ribes magellanicus* (Grossulariaceae), *C. diffusum* (Asteraceae), *E. serrata, Empetrum rubrum* (Escalloniaceae), *Maytenus disticha* (Celastraceae), and *Em. coccineum* (Proteaceae). The herbaceous understory is dominated by *Acaena ovalifolia* (Rosaceae), *Ozmorhiza obtusa* (Apiaceae), *Cardamine glacialis* (Brassicaeae), and the fern *B. penna-marina* (Blechnaceae).
3) Patagonian steppe. This vegetation unit occurs in areas where the mean annual precipitation is <400 mm. The dominant species is *Festuca gracillima*, along with *Festuca magallanica, Stipa brevipes, Bromus unioloides* (Poaceae), *Acaena argentea, Acaena intergerrima, Acaena pinnatifida* (Rosaceae), *Adesmia pumila* (Papilionaceae), and *Arjona patagonica* (Santalaceae). Common shrubs in this unit are *Adesmia boronoides, Berberis buxifolia, Berberis empetrifolia*, *C. diffusum, Baccharis magallanica* (Asteraceae), *Mulinum spinosum* (Apiaceae), and *Verbena tridens* (Verbenaceae).
4) Andean desert. This sparsely vegetated unit occurs above the *Nothofagus* forests and includes small patches of *N. pumilio* and dwarf shrubs such as *Escallonia rubra* and *Ribes cuccullatum.* The predominantly herbaceous cover is dominated by *Acaena magallanica, Pernettya pumila* (Ericaceae), *Empetrum rubrum* (Empetraceae), *Senecio skottbergii* (Asteraceae), *Leuceria leonthopodioides* (Asteraceae), *Perezia megalantha* (Asteraceae), *Nassauvia lagascae* (Asteraceae), *Agrostis canina* (Poaceae), and *Festuca pyrogea.*

2. Materials and methods

We obtained multiple overlapping sediment cores from the deepest sectors of Pantano Dumestre (51°48′13.83″S, 72°26′9.15″W, 77 m.a.s.l.) and the Eberhard site (51°34′36.98″S, 72°40′4.27″W, 68 m.a.s.l.) using a 5-cm diameter Wright piston corer. Both sites are small closed basins located on bedrock depressions in the gently sloping low-lying terrain (<150 m.a.s.l.) that develops east of Seno Última Esperanza and Golfo Almirante Montt and west of Sierra Dorotea and the Arauco moraine complex (Fig. 1). The landscape surfaces are mantled with glaciolacustrine mud, ice-rafted detritus (below 150 m.a.s.l.), cobbles and occasional large boulders, attesting for a former glacial and glaciolacustrine cover. Pantano Dumestre is a seasonally dry elliptical *Sphagnum* bog (1300 m × 550 m), located just east of Golfo Almirante Montt ~9 km SE of Puerto Natales. The bog has undergone considerable surface and subsurface burning along its periphery; signs of disturbance are also evident along the surrounding slopes in the form of erosion and abundant scorched logs and branches. We cored the central area of the bog having the thickest accumulation of peat and lake sediments, which we determined after conducting a depth survey that encompassed the entire length and width of the site. The depth measurements were performed using stainless steel probe rods at regular 10-m intervals along transects on the bog surface. The Eberhard site includes a small lake surrounded by a bog, located next to a ~20-m high, N–S oriented glacially scoured bedrock knob in an area adjacent to Puerto Consuelo, ~21 km northwest from Puerto Natales. We obtained sediment cores from the middle portion of the lake using an anchored raft equipped with a 10-cm wide aluminum casing, following a bathymetry study of the lake with a sonar. We also retrieved sediment cores from a bog adjacent to the western side of the lake, in a sector that contained the thickest sediment package as determined by a depth survey we conducted prior to coring.

The stratigraphy of the cores was characterized by lithological descriptions, digital X-radiographs, and loss-on-ignition analysis following overnight drying at 105 °C. We performed sequential burns at 550 °C for 2 h (LOI_{550}) and 925 °C for 4 h (LOI_{925}) in a muffle furnace to quantify the organic and carbonate content of the sediments, respectively (Bengtsson and Enell, 1986; Heiri et al., 2001). Identification and correlation of tephras with known eruptions of specific source volcanoes in the region (Stern, 2008) were based on petrology and trace-element chemistry determined by ICP-MS analysis. Geochemical and radiocarbon data on the R1 tephra can be found in Sagredo et al. (2011) and Stern et al. (2011). Detailed examination of the carbonate layers found in the Lago Eberhard core was carried out using the scanning electron microscope facility at the University of Geneva (D. Aritztegui, pers. comm.). The chronology of the sediment cores is controlled by AMS radiocarbon dates obtained from 1-cm thick sections along the cores. All radiocarbon dates were converted to cal yr BP using the IntCal09 calibration curve included in the CALIB 6.0 software (Reimer et al., 2009). Based on these data we developed age models to assign interpolated calendar ages to the levels analyzed, using

cubic splines produced by the R software (R Development Core Team, 2010).

We processed 2 cc sediment samples for pollen analysis using standard techniques that include KOH deflocculation, concentrated HF treatment, and acetolysis (Faegri and Iversen, 1989). We added *Lycopodium* spore tablets to the sediment samples to allow calculation of pollen and charcoal concentration and accumulation rates. The concentrates were mounted on glass slides in a silicon oil (2000 cs) mounting medium and analyzed at 400× and 1000× magnification using a Leica DMLB2 and a Zeiss Axioscop 40 stereomicroscope. We counted the pollen and spore content of these samples considering a minimum of 300 grains of terrestrial origin per level, and calculated their percent abundance as a function of this pollen sum. In the case of aquatic plants and ferns we calculated percentages in reference to sums that included all pollen grains (terrestrial and aquatic) and spores, respectively. The percent abundance of the microalga *Pediastrum* was calculated on the basis of another sum that included all pollen, spores, and microalgae. Definition of the pollen zones is based on visual inspection and detection of the major changes in the pollen stratigraphy, supported with a stratigraphically constrained CONISS ordination. For that purpose we considered only the terrestrial taxa with abundance ≥2%, and then recalculated sums and percentages.

We analyzed the macroscopic charcoal content of 2-cc sediment samples taken at contiguous 1-cm thick intervals using the methodology described by Whitlock and Anderson (2003), which includes deflocculation with 10% KOH and sieving through 106-μm and 212-μm mesh screens. We counted charcoal particles in each size class under a Zeiss KL1500 LCD stereomicroscope at 50–100× magnification, and distinguished as "herbaceous charcoal" from "undifferentiated charcoal" whenever possible depending on their preserved macroscopic anatomy. These data are expressed as % herbaceous charcoal. The abundance of macroscopic charcoal particles is expressed as charcoal accumulation rate (CHAR). We performed time series analysis of the charcoal data using the CharAnalysis software described by Higuera et al. (2009), interpolating samples at regular intervals defined by the median time resolution of each record. We decomposed CHAR into background and signal components using a lowess robust to outliers and smoothing windows of variable length for each record. We separated charcoal peaks from the background noise using a Gaussian mixture model to estimate the mean and variance of the noise distribution. Charcoal peaks, interpreted as local fire events, were identified as interpolated accumulation-rate values exceeding the 99th percentile of the noise distribution.

3. Results

3.1. Stratigraphy and chronology

3.1.1. Pantano Dumestre

We retrieved Wright core PS0607A which starts 100 cm below the bog surface and has a length of 766 cm. This was accompanied by an overlapping core, PS0607B, obtained 2 m apart which covers the depth range between 150 and 450 cm. Each core was sampled continuously for LOI to allow cm-scale correlations with the aim of producing a spliced record devoid of hiatuses associated with core breaks in the upper portion of the record. The record shows a basal minerogenic unit with millimeter-scale laminations of silts, clays, occasional sand layers and angular granule- and pebble-sized clasts (core PS0607A) (Figs. 2 and 3). An abrupt concordant transition gives way to organic sediments, featuring a basal coarse organic detritus gyttja unit with high organic content (LOI_{550} > 50%) and abundant remains of peat mosses. Within this peat we found two tephras derived from Volcán Reclús (380–400 cm) separated by four centimeters of peat. The sediments then shift to faintly laminated, strongly banded organic silts between 263 and 366 cm, the lower portion of which has a fairly homogeneous organic content of 21.8 ± 0.6% (mean ± standard deviation, LOI_{550}), followed by a brief reversal to a fibrous, plant-debris rich bed with high organic content (47 ± 9.9% between 326 and 331 cm) and overlain in turn by silts with low organic content (11.6 ± 2.4% between 263 and 326 cm). The sediments then turn to coarse organic detritus gyttja between 250 and 263 cm and then to fibrous peat that persists until

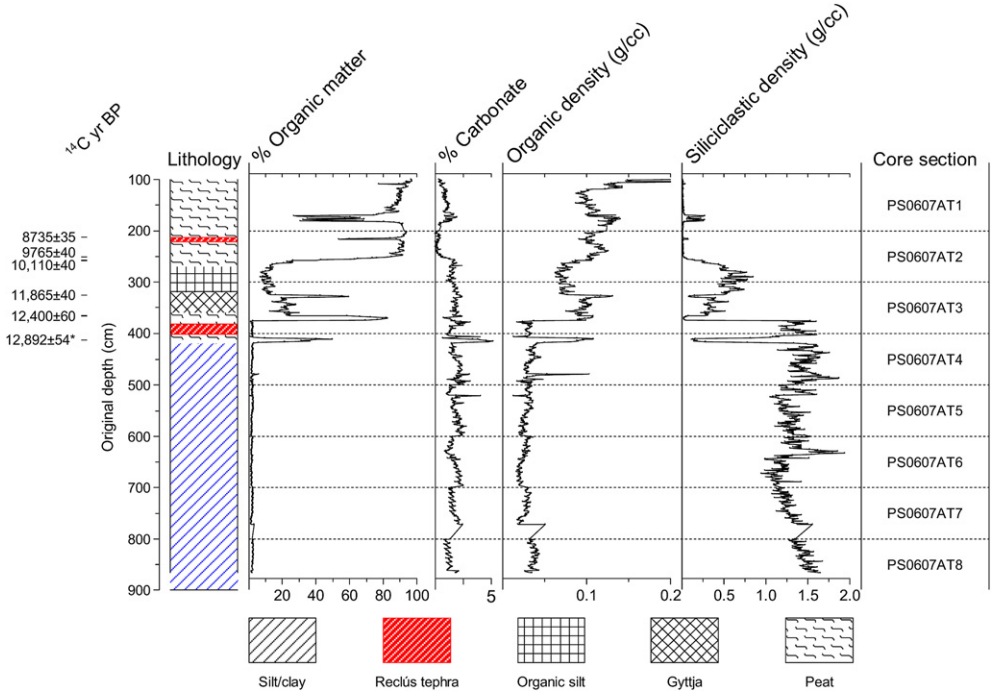

Fig. 2. Stratigraphic column, radiocarbon dates and loss-on-ignition data of core PS0607A from Pantano Dumestre.

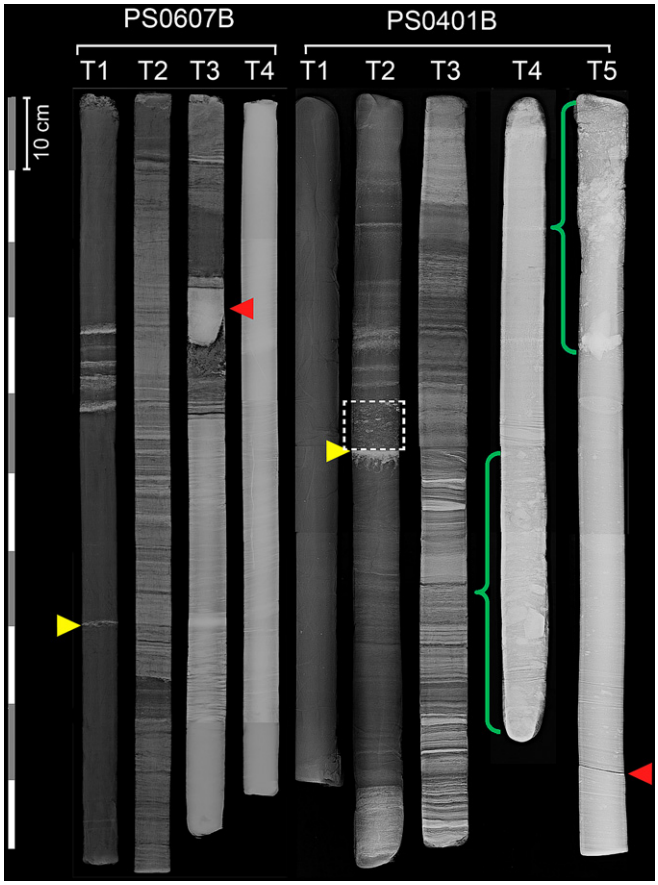

Fig. 3. Digital X radiographs from the upper part of cores PS0607A (left) and PS0401B (right) obtained from Pantano Dumestre and Lago Eberhard, respectively. The individual cores are aligned from left to right in descending order with the core tops oriented upward. The dashed white rectangle indicates an oblique fining-upward clastic sequence which we interpret as an unconformity. The curly green brackets indicate an IRD-enriched zone of the glaciolacustrine unit found in the Lago Eberhard cores.

the modern surface of the bog. Within the peat unit we found a 2-cm thick tephra from Volcán Reclús (215–216 cm) (C. Stern, pers. comm.) and a series of clastic layers between 170 and 183 cm.

We obtained 10 AMS radiocarbon dates from the Pantano Dumestre cores (Table 1), three of which were retrieved from the base of the organic deposits, in an effort to pinpoint the transition from laminated silts and clays to organic sediments with precise close-minimum limiting ages. The latter dates yielded statistically the same age for the onset of organic accumulation, with a weighted mean of 12,892 ± 27 ^{14}C yr BP (median probability: 15,375 cal yr BP). Successively younger ages further up in the stratigraphy demonstrate continuous in-situ accumulation of peat overlain by organic silts starting at 12,400 ± 60 ^{14}C yr BP (median probability: 14,457 cal yr BP), which grade to silts with low organic content at 11,820 ± 45 ^{14}C yr BP (median probability: 13,676 cal yr BP), overlain by coarse organic detritus gyttja superseded by fibrous peat. The latter transition occurs between 10,050 ± 45 and 9765 ± 40 ^{14}C yr BP (median probabilities: 11,563 and 11,151 cal yr BP, respectively). One date at 212 cm depth yielded a close maximum limiting age of 8735 ± 35 ^{14}C yr BP (median probability: 9624 cal yr BP) for the upper Reclús tephra. Two dates obtained in the organic silts section at 281 and 311 cm yielded spurious results and were excluded from the age model.

Several fast-sediment accumulating closed-basin lakes and bogs from the Última Esperanza and Torres del Paine region contain an early Holocene tephra erupted from Volcán Reclús (Stern, 2008). Six radiocarbon dates obtained in direct contact with this ash yielded statistically the same age, with a weighted mean of 9320 ± 15 ^{14}C yr BP (median probability: 10,540 cal yr BP) (Table 2). We developed an age model to assign interpolated calendar ages to the pollen and charcoal levels of core PS0607A (Fig. 3) based on the radiocarbon dates discussed above and the weighted mean for the upper tephra from Volcán Reclús. The age model consists of a cubic spline function with a weighting of 0.15, and takes into account the instantaneous deposition of tephra layers by subtracting their thickness from the depth of the radiocarbon dates and pollen/charcoal levels.

3.1.2. Eberhard site

We retrieved sediment cores PS0301A (780 cm long) and core PS0301B (790 cm long) from a bog adjacent to Lago Eberhard, of these we chose core PS0301A to conduct LOI analysis and obtain radiocarbon dates, based on its stratigraphic completeness and optimal recovery. Four main stratigraphic units characterize core PS0301A: basal pebbly mud, overlain by an abrupt concordant transition to organic mud (gyttja), then coarse organic detritus mud (gyttja), capped by silty peat on the upper part of the record (Fig. 4). We found two distinct tephras from Volcán Reclús (R1 tephras) immersed in the upper portion of the pebbly mud unit (between 550 and 560 cm). The fact that these tephras are separated by 3 cm of silty clays suggests that they represent discrete ashfall events. The upper portion of the pebbly mud unit, bounded by the R1 tephras and the onset of organic sedimentation (between 526 and 550 cm), contains a conspicuously high abundance of sharp-edged, granule to pebble-sized lithic fragments. A third Reclús tephra is present higher up in the stratigraphy at 384 cm depth (C. Stern, pers. comm.).

We also obtained sediment cores from the lake centre (337 cm water depth) using an anchored raft equipped with a 10-cm wide aluminum casing. Here we retrieved multiple overlapping cores and selected core PS0401B considering its stratigraphic completeness and optimal recovery, also because it replicates important aspects of the stratigraphy documented in the bog cores (Figs. 3 and 4). Three aspects, however, differ between cores PS0401B and PS0301A: (i) the PS0401B record shows predominance of organic-rich lacustrine sediments and lack of peat deposits, (ii) the presence of millimeter and centimeter-thick low-Mg authigenic calcite laminae with well-developed crystal shapes and framboidal pyrite crystals (D. Ariztegui, pers. comm.) in the lower portion of organic mud (between 548 and 660 cm), (iii) higher sediment-accumulation rates between R1 (between 840 and 844 cm) and the upper Reclús tephra (509–512 cm). The latter factor permitted the development of high-resolution pollen and macroscopic charcoal records based of continuous-contiguous 1 cm-thick samples. Moreover, the higher sedimentation rate during this interval allows a better characterization of the pebbly mud unit located between the R1 tephras and the onset of organic sedimentation in multiple lake cores, including PS0401B (between 663 and 840 cm) (Fig. 5, Table 1).

We obtained six AMS radiocarbon dates from core PS0301A, two of them were obtained from organic laminae within the pebbly mud unit at 728 cm (13,745 ± 50 ^{14}C yr BP, median probability: 16,373 cal yr BP) and 674 cm (13,690 ± 45 ^{14}C yr BP, median probability: 16,305 cal yr BP), three other come from the base of the organic mud unit between 521 and 524 cm (weighted mean: 10,462 ± 24 ^{14}C yr BP, median probability: 12,432 cal yr BP), and another date higher up in the stratigraphy (383 cm depth) underlying the upper Reclús tephra (9435 ± 35 ^{14}C yr BP, median probability: 10,667 cal yr BP) (Table 1). This date shows good agreement with several radiocarbon dates obtained from other sites having

Table 1
Radiocarbon dates from Pantano Dumestre and the Eberhard site. The calibrated ages were obtained using the intcal09 calibration dataset contained in Calib 6.0.2 (Reimer et al., 2009).

Laboratory code (CAMS#)	Core	Depth (cm)	$\delta^{13}C$ ‰	^{14}C yr BP	1 σ Error	Median probability (cal yr BP)	Lower 2 σ intercept (cal yr BP)	Upper 2 σ intercept (cal yr BP)
133256	PS0607AT2	212	−25	8735	35	9624	9540	9742
137862	PS0607AT2	250	−25	9765	40	11,151	10,822	11,235
128992	PS0607AT2	257	−25	10,050	45	11,563	11,329	11,807
129004	PS0607AT3	325	−25	11,820	45	13,676	13,474	13,807
128993	PS0607AT3	365	−25	12,400	60	14,457	14,098	14,960
129005	PS0607AT4	416	−25	12,875	45	15,360	15,007	15,903
125918	PS0607AT4	418	−25	12,910	50	15,417	15,040	16,065
129006	PS0607BT3	382	−25	12,895	45	15,389	15,017	16,041
	Weighted mean	417		12,892	27	15,375	15,035	15,901
98919	PS0301AT4	384	−25	9435	35	10,667	10,577	10,749
98830	PS0301AT5	518	−27	10,525	45	12,534	12,380	12,731
107006	PS0301AT5	521	−25	10,535	40	12,550	12,388	12,709
107007	PS0301AT5	524	−25	10,340	40	12,184	12,034	12,384
98831	PS0301AT7	675	−27	13,690	45	16,305	15,964	16,703
107008	PS0301AT7	728	−25	13,745	50	16,373	16,022	16,762
124565	PS0401BT2	490	−27.8	5810	20	6553	6469	6641
107051	PS0401BT2	547	−25	9980	35	11,415	11,268	11,611
115805	PS0401BT3	565	−26	9920	40	11,312	11,229	11,599
	Weighted mean	556		9954	53	11,345	11,253	11,600
115811	PS0401BT3	565	−25	9615	35	10,937	10,780	11,167
115810	PS0401BT3	610	−25	10,490	40	12,507	12,239	12,683
107052	PS0401ET1	662	−25	10,695	40	12,769	12,680	12,828

similar depositional settings (see discussion above and Table 2). We obtained five radiocarbon dates from lake cores PS0401BT3 and PS0401ET1, the lowermost of which affords a close minimum limiting age for the onset of organic sedimentation in the site of 10,695 ± 40 ^{14}C yr BP (median probability: 12,769 cal yr BP), followed in stratigraphic sequence by younger dates. We developed an age model based on a cubic spline function with a weighting of 0.1 to assign interpolated calendar ages to the pollen and charcoal levels of core PS0401B (Fig. 3). The age model takes into account the age of R1 and the radiocarbon ages from the lake cores excluding the date 9615 ± 35 ^{14}C yr BP, considering that it is anomalously young. The age model takes into account the weighted mean age of dates 9980 ± 35 and 9920 ± 40 ^{14}C yr BP, considering they were statistically identical at 2 sigma range, and the weighted mean age for the upper Reclús tephra discussed above.

3.2. Fossil pollen

3.2.1. Pantano Dumestre

We analyzed 93 palynological levels from core PS0607A between 200 and 355 cm depth, spanning the time interval between ~10,000 and 14,300 cal yr BP with a median time resolution of 28 years between levels. Samples below 355 cm contained extremely low pollen and spore concentrations to yield representative samples to be incorporated in the description/discussion. The palynological results are shown in percentage diagrams (Fig. 6) which depict the pollen assemblage zones we defined on the basis of conspicuous changes in the pollen stratigraphy and a CONISS ordination. In the following paragraphs we provide a brief description of each pollen zone, defined by the three most abundant terrestrial plant taxa in decreasing order of mean abundance. We specify the mean percentages of relevant taxa in parenthesis whenever useful.

Zone PD1 (328–355 cm, ~13,850–14,250 cal yr BP). The assemblage *Acaena*–Poaceae–Asteraceae subfamily Asteroidea dominates this zone along with the shrubs *Empetrum rubrum* (5.8%) and Ericaceae (2%). The aquatic angiosperm *Myriophyllum* (56.4%) reaches its all-time maximum, accompanied by the green microalga *Pediastrum* (53.2%) which shows highly variable percentages. The arboreal taxon *Nothofagus dombeyi* type (6.1%), the fern *Blechnum* (5.1%) and Cyperaceae (3.1%) exhibit their lowest abundance in the entire record.

Table 2
Close maximum limiting ages for an early-Holocene Reclús tephra found in several fast-sediment accumulating closed-basin lakes and bogs from the Última Esperanza and Torres del Paine area. We calculated a weighted mean of 9320 ± 15 ^{14}C yr BP (median probability: 10,540 cal yr BP) for the deposition of this tephra.

Laboratory code (CAMS#)	Site name	Coordinates	Core	Depth (cm)	^{14}C yr BP	1 σ Error	Median probability (cal yr BP)	Lower 2 σ intercept (cal yr BP)	Upper 2 σ intercept (cal yr BP)
98919	Pantano Eberhard	51°34′36.98″S, 72°40′4.27″W	PS0301AT4	383–384	9435	35	10,610	10,501	10,713
98829	Vega Benítez	51°33′40.20″S, 72°35′7.32″W	PS0302AT4	366–367	9145	40	10,241	10,183	10,383
98918	Vega Benítez	51°33′40.20″S, 72°35′7.32″W	PS0302AT4	367–368	9130	35	10,231	10,177	10,367
98835	Vega Ñandú	50°55′59.26″S, 72°46′10.98″W	PS0304AT3	312–314	9310	40	10,428	10,275	10,561
99122	Vega Ñandú	50°55′59.26″S, 72°46′10.98″W	PS0304AT3	312–314	9430	35	10,603	10,445	10,712
131269	Lago Cipreses	51°17′6.15″S, 72°51′13.48″W	PS0710AT3	305–306	9435	40	10,609	10,444	10,726
			Weighted mean		9316	15	10,535	10,442	10,577

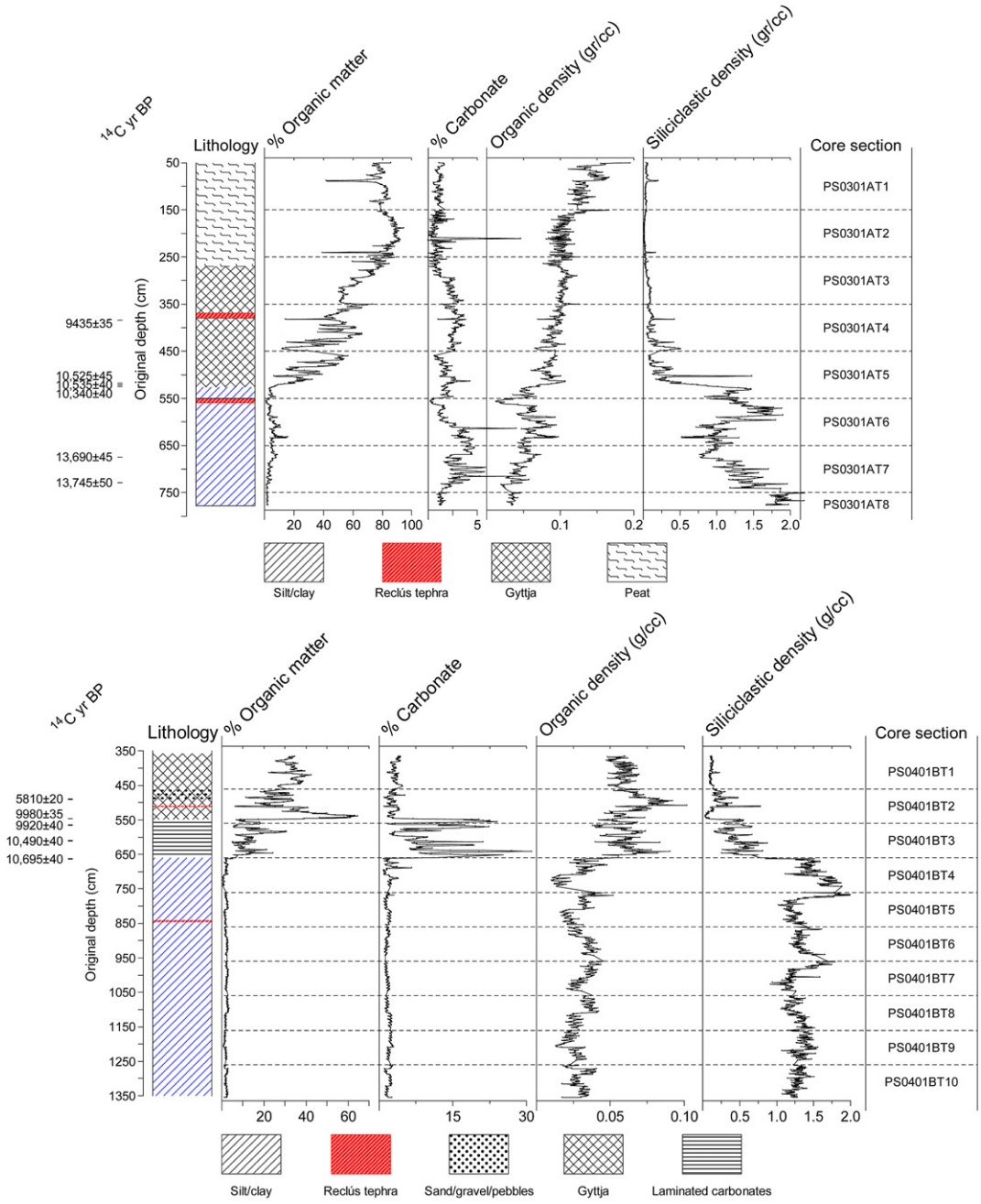

Fig. 4. Stratigraphic column, radiocarbon dates and loss-on-ignition data of cores PS0301A and PS0401B from Pantano Eberhard and Lago Eberhard, respectively.

Zone PD2 (305–328 cm, ~13,200–13,850 cal yr BP). This zone features the *Acaena*-Poaceae-*N. dombeyi* type assemblage, the appearance of *Misodendron* (a hemi-parasite on species of the genus *Nothofagus*) and *Galium* type (3.6%) in the record, and declines in Asteraceae subfamily Asteroidea (1.4%), *Empetrum* (1%), and Ericaceae (<1%). The most remarkable change during this zone is an abrupt decline in *Myriophyllum* (17.3%), coeval with a rise in *Blechnum* (20.1%), *Pediastrum* (60.1%) and arboreal pollen (from 6.3% to 14.5%). Cyperaceae persists in low abundance (4.2%).

Zone PD3 (288–305 cm, ~12,600–13,200 cal yr BP) features the Poaceae–*N. dombeyi* type–*Acaena* assemblage, increments in *Galium* type (9.8%) and *Pediastrum* (76.1%), and consistently low abundance of *Myriophyllum* (11%) and Cyperaceae (5.2%).

Zone PD4 (257–288 cm, ~11,500–12,600 cal yr BP). Two large-magnitude increments in *Galium* type lead to the *Galium* type-Poaceae-*N. dombeyi* type assemblage, and declines in other herbs. *Myriophyllum* increases slightly (14%) while *Pediastrum* (76.2%) and *Blechnum* (24.7%) remain at their maximum abundance, and Cyperaceae persists in low abundance (3.1%).

Zone PD5 (200–257 cm, ~10,000–11,500 cal yr BP). An abrupt decline in *Galium* type (from 70.8% to <1% in 200 years [5 cm]) and rapid increases in Poaceae and *N. dombeyi* type led to the establishment of the Poaceae–*N. dombeyi* type–*Acaena* assemblage. Cyperaceae exhibits a 10-fold increase in 200 years (5 cm), concurrent with declines in *Myriophyllum* (<1%) and *Pediastrum* (3.1%). The latter taxon declined rapidly from its peak abundance (90.6%) to <1% in 350 years (10 cm).

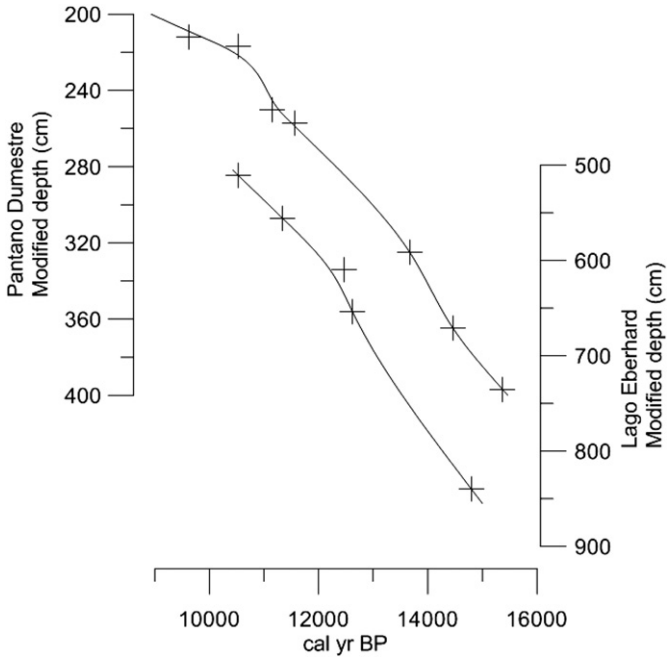

Fig. 5. Age/depth curves and age models applied to cores PS0607A and PS0401B. Notice the modified depth *y* axes (cal kyr BP = 1000 cal yr BP).

3.2.2. Eberhard site

We analyzed 148 palynological levels between 512 and 655 cm depth in core PS0401B, which correspond to the time interval between ~10,600 and 12,800 cal yr BP. The resulting pollen record has a median time resolution of 15 years between samples. We did not include the palynological results of samples located below 655 cm because they contained extremely low pollen and spore concentrations to yield representative counts. The palynological results and assemblage zones are shown in percentage diagrams (Fig. 7). In the following paragraphs we describe the pollen zones, which we named on the basis of the four most abundant terrestrial plant taxa. The lower three zones (LE1A, LE1B, and LE1C) share the same hierarchical sequence of the four most abundant palynomorphs, but exhibit conspicuous variations on the abundance of these dominant taxa and distinct changes in other plant taxa.

Zone LE1A (619–655 cm, ~12,300–12,800 cal yr BP). This zone is dominated by the Poaceae–*N. dombeyi* type–*Acaena*–Asteraceae subfamily Asteroidea assemblage, accompanied abundant *Myriophyllum* (7.1%) and Caryophyllaceae (2.2%), along with traces (<1%) of *Moscharia* and *Valeriana*. *Myriophyllum* achieves its maximum abundance in the lowest part of the record (mean: 15% between ~12,600 and 12,800 cal yr BP) and declines rapidly thereafter.

Zone LE1B (579–619 cm, ~11,800–12,300 cal yr BP). The assemblage Poaceae–*N. dombeyi* type–*Acaena*–Asteraceae subfamily Asteroidea persists during this zone with a slight increase in *N. dombeyi* type (from 7.2 to 11.1%), a gradual and sustained rise in *Blechnum* (from <1 to 3.9%), a major decline in *Myriophyllum* (<1%) and subtle decreases in Caryophyllaceae, *Moscharia*, and *Valeriana*.

Zone LE1C (566–579 cm, ~11,300–11,800 cal yr BP). The Poaceae–*N. dombeyi* type–*Acaena*–Asteraceae subfamily Asteroidea assemblage prevails during this zone with a conspicuous decline in Poaceae (73.3–60.1%), a modest rise in *N. dombeyi* type (from 7.2 to 11.1%), an abrupt increase in *Plantago*, and a steady increase in *Blechnum*. *Plantago* shows centennial-scale variations in its abundance.

Zone LE2 (512–556 cm, ~10,600–11,300 cal yr BP). A major change in the pollen record led to the *N. dombeyi* type–Poaceae–*Acaena*–*Plantago* assemblage, which is accompanied by an increase in *Misodendron* (2%), peak abundance of arboreal pollen (62.7%) and *Blechnum* (24.7%). *N. dombeyi* type rose from <15% to >60% in 250 years (15 cm), accompanied by abrupt declines in Poaceae and *Acaena*.

3.3. Fossil charcoal

3.3.1. Pantano Dumestre

We developed a macroscopic charcoal record from continuous/contiguous 1-cm thick levels between 200 and 377 cm from core PS0607A, having a median time resolution of 28 years between samples (Fig. 8). CHAR (Charcoal Accumulation Rates) are extremely low between 326 and 378 cm (~13,700–14,800 cal yr BP), followed by a moderate increase between 253 and 326 cm (~11,400–13,700 cal yr BP), a highly variable rise between 226 and 253 cm (~10,700–11,400 cal yr BP), and a gradual and variable decline between 200 and 226 cm (~8900–10,700 cal yr BP). Herbaceous charcoal is most abundant (mean: 32.8%) between 247 and 325 cm (~11,200–13,700 cal yr BP), after which it declines to a minimum (~5%) over an interval of ~1300 years. Time series analysis and local fire detection of these data using the CharAnalysis software (Fig. 8) revealed 11 statistically significant peaks (global Signal to Noise Index [SNI] = 0.58) with maximum frequency of events at ~13,300 cal yr BP, a steady decline until ~11,700 cal yr BP, multi-centennial scale fluctuations with a rise until ~11,100 cal yr BP followed by a decline to a minimum at ~10,700 cal yr BP, and a persistent though variable increase until ~8900 cal yr BP.

3.3.2. Lago Eberhard

Contiguous 1-cm thick sampling and analysis of core PS0401B between 512 and 655 cm depth yielded a macroscopic charcoal record having a median time resolution of 15 years between samples (Fig. 8). The CHAR curve shows peak abundance between 601 and 648 cm (~12,400–12,600 cal yr BP) followed by a highly variable and gradual decline between 505 and 601 cm (~10,400–12,400 cal yr BP). The proportion of herbaceous charcoal remains high with little variation (mean: 76.3%) below 550 cm (>11,300 cal yr BP) and declines abruptly (<20 years) to minimum values between 505 and 550 cm (mean: 17.3%). The CharAnalysis software detected 11 statistically significant peaks (global SNI = 0.81) with a rise in fire frequency between ~10,900 and 11,600 cal yr BP and prominent declines between ~10,500–10,900 and ~11,600–12,700 cal yr BP (Fig. 8).

4. Discussion

4.1. Stratigraphy and chronology

Sediment cores from Pantano Dumestre and the Eberhard site record environmental changes in the lowlands adjacent to Golfo Almirante Montt and Seno Última Esperanza since the local retreat of the Patagonian Ice Sheet from its LGM limit. These records reveal >5 m of a basal minerogenic unit with varying degrees of stratification (Figs. 2 and 4), ranging from well-sorted silts and clays exhibiting millimeter-scale horizontal laminations to large angular clasts embedded in a massive matrix of silt, sand and gravel (Fig. 3). We interpret these deposits as glaciolacustrine mud containing varying amounts of laminated silts and clays to massive Ice Rafted Debris (IRD), ranging in size from granule to large angular pebbles, deposited in the bottom of glacial lake Puerto Consuelo (Sagredo et al., 2011).

Glaciolacustrine sedimentation began in the lowlands (<125 m.a.s.l.) adjacent to Golfo Almirante Montt and Seno Última Esperanza when the eastern margin of the Última Esperanza piedmont lobe abandoned a stabilized position distal to the

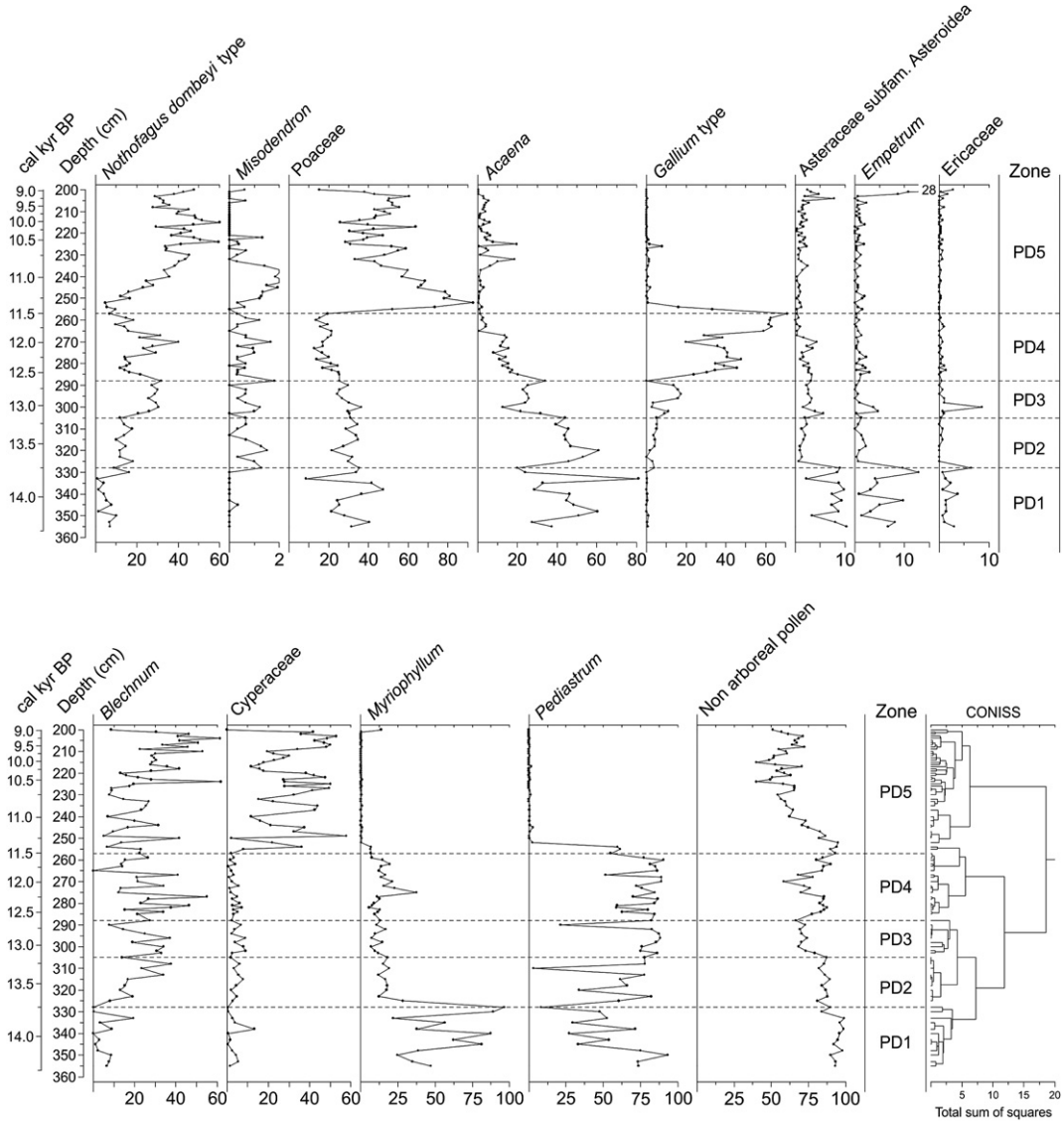

Fig. 6. Percentage diagrams of pollen and spores from Pantano Dumestre (core PS0607A).

Pantano Dumestre and the Eberhard site and the Lago Pinto Moraine complex during the last glacial termination (Sagredo et al., 2011), leading to the enlargement and surface lowering of glacial lake Puerto Consuelo. Radiocarbon dates retrieved from organic laminae found in the basal glaciolacustrine unit of core PS0301A from Pantano Eberhard, underlying the R1 tephras, yielded identical ages of ~16,400 cal yr BP, which we interpret as minimum limiting ages for local ice-free conditions and development of the ice-dammed lake. Glaciolacustrine sedimentation ended abruptly and gave way to subaqueous deposition of organic material in Pantano Dumestre and the Eberhard site (Figs. 2–4), respectively, implying local regressions of glacial lake Puerto Consuelo. Our radiocarbon chronology indicates that the Pantano Dumestre basin was exposed to sub-aerial conditions by ~15,380 cal yr BP and the Lago Eberhard basin by ~12,800 cal yr BP (Figs. 2 and 4, Table 1). Considering that both sites are located only 30 km apart, less than 3 km from the modern coastline (Fig. 1), and within the same glacial morphostratigraphic position, we interpret this chronological difference as variations in the surface elevation of glacial lake Puerto Consuelo, and rule out that these differences are related to isostatic adjustments during the last glacial termination (Sagredo et al., 2011). Multiple field measurements using a hand-held GPS, immediately following altitudinal calibrations at sea level, gave elevations of ~80 m.a.s.l. for the surface of Pantano Dumestre and ~70 m.a.s.l. for the Eberhard site. Although both altitudes overlap within the error range for the instrument, we think the difference of ~10 m in elevation is genuine and can account for the difference in timing for the onset of organic sedimentation. We note that both sites contain the R1 tephras, in the case of Pantano Dumestre they are found in peat/coarse detritus gyttja whereas in the Eberhard site it is immersed in glaciolacustrine sediments, supporting the interpretation that glacial lake Puerto Consuelo persisted at elevations between 70 and 80 m.a.s.l. in the interval dated between ~12,800 and 15,380 cal yr BP.

The x radiographs and inorganic density data from all cores collected in Lago Eberhard indicate a sustained and conspicuous peak in IRD (Figs. 3 and 4), which Sagredo et al. (2011) interpreted as the distal expression of a glacial readvance into glacial lake Puerto Consuelo. Those authors considered the Antonio Varas Moraine Complex (Fig. 1) as a likely candidate for the ice margin of the Última Esperanza lobe during this readvance. Based on an interpolation between the age of the R1 tephras and close

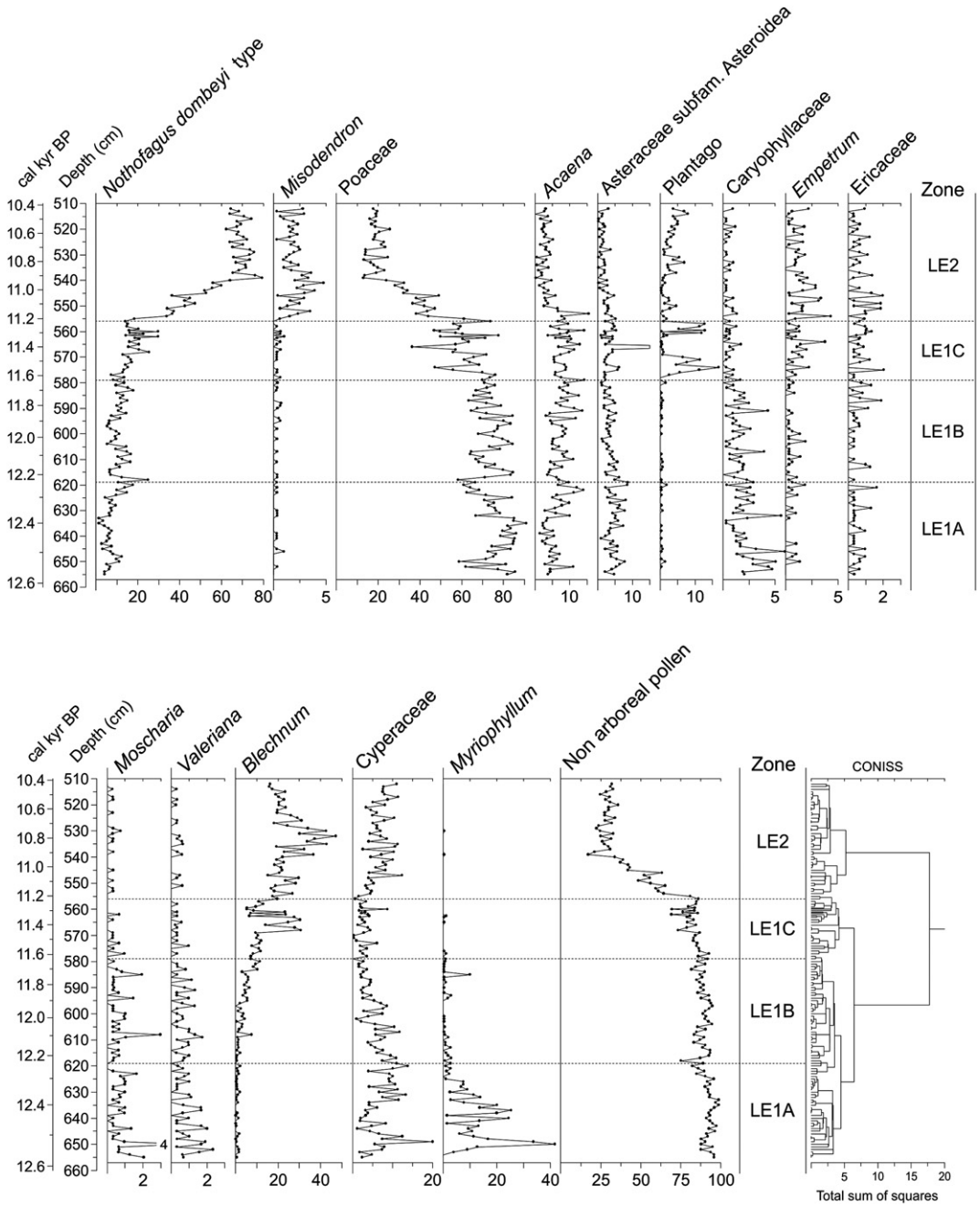

Fig. 7. Percentage diagrams of pollen and spores from Lago Eberhard (core PS0401B).

minimum limiting radiocarbon dates for the onset of organic sedimentation in core PS0401B, we bracket the deposition of the IRD-enriched zone between ~13,100 and 13,600 cal yr BP in core PS0401B (Fig. 5, Table 1). The timing for its onset and culmination should be considered a first approximation given that the R1 tephra and the nearest radiocarbon dates from the overlying organic mud do not provide the closest possible bracketing age controls in the sediments cores from Lago Eberhard.

The lithostratigraphy from Pantano Dumestre indicates a shallow closed-basin lake between ~14,900 and 15,380 cal yr BP which became a peatland (Figs. 2 and 3) between ~14,600 and 14,900 cal yr BP, marking terrestrialization of the lake. This was followed by a shift to organic silts and disappearance of peat mosses that we interpret as a reversal back into a subaqueous depositional environment, suggesting a transgressive lake-level phase between ~11,600 and 14,600 cal yr BP. This trend was punctuated by a brief reversal between ~13,600 and 13,700 cal yr BP, evident in the lithostratigraphy and loss-on-ignition data as a rapid increase in the % organic matter between 326 and 331 cm depth (Fig. 2). The sediments shift to shallow organic lake deposits at ~11,800 cal yr BP and then to Cyperaceae-*Sphagnum* peat by ~11,500 cal yr BP, marking terrestrialization of the site that has persisted during the entire Holocene.

Piston cores from the Eberhard basin, on the other hand, record sedimentation in a small closed-basin lake, disconnected from glacial lake Puerto Consuelo, starting at ~12,800 cal yr BP (Figs. 3 and 4). Organic-rich lake sediments have accumulated in the lake's center with little variation since then, except for an interval

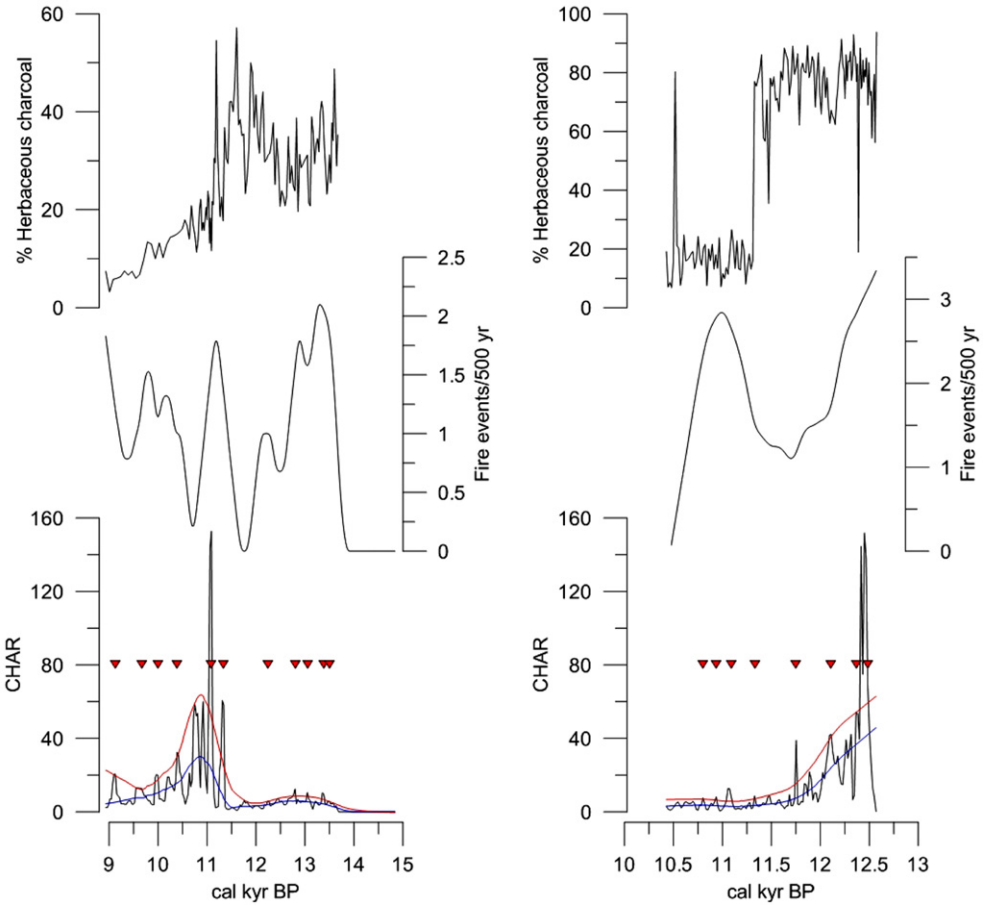

Fig. 8. Results of the macroscopic charcoal analysis from cores PS0607A (left) and PS0401B (right). Also shown are the results of the time series analysis performed with the program CharAnalysis. The blue lines represent the calculated background using a lowess robust to outliers, the red line represents the locally defined threshold, and the triangles represent the statistically significant charcoal peaks.

with laminated authigenic calcite between ~11,600 and 12,800 cal yr BP, and an erosive interval presumably related to a lower stand sometime between ~6600 and 10,600 cal yr BP. Sediment infill in the periphery led to terrestrialization of its western margin and development of a swamp and minerotrophic fen which persist until present.

4.2. Vegetation and fire history

The Pantano Dumestre record shows persistently high abundance of the planktonic alga *Pediastrum* between ~11,500 and 14,600 cal yr BP concurrent with lacustrine sedimentation at the site, suggesting a permanent water body (Fig. 9). During this interval we observe dominance of cold-resistant herbs (*Acaena*, Poaceae, Asteraceae subfamily Asteroidea, *Galium* type) accompanied by *N. dombeyi* type and the shrubs *Empetrum rubrum* and Ericaceae. *Galium* type rose abruptly between ~11,600 and 13,100 cal yr BP while most herbs declined and *N. dombeyi* type started an oscillating increase with maxima between ~12,600–13,000 and ~11,800–12,200 cal yr BP (Fig. 9). Within the lacustrine phase we detect a relatively shallow lake interval between ~13,600 and 14,600 cal yr BP based on the predominance of horizontally lain organic silts (Figs. 2 and 3) and abundant *Myriophyllum* pollen (Fig. 9), a submerged macrophyte that today grows at depths ≤4 m in the littoral zone of lakes located in the humid regions of western Patagonia. We interpret these results as the local occurrence of this littoral macrophyte in the deepest part of the lake between ~13,600 and 14,600 cal yr BP. A deeper lake phase ensued between ~11,600 and 13,600 cal yr BP (Fig. 9) judging from a major decline of *Myriophyllum* pollen in the context of persistently high *Pediastrum* and sedimentation of horizontally lain silts with a lower organic content (Figs. 2, 3 and 6), all indicative of outward migration of littoral environments and a deeper depositional environment in the center of the lake in response to a lake level rise.

Pantano Dumestre records abrupt declines in *Galium* type, *Pediastrum*, and *Myriophyllum* starting at ~11,600 cal yr BP, contemporaneous with rapid increases in Poaceae and Cyperaceae and a transition from organic silts through coarse organic detritus gyttja to fibrous peat (Fig. 9). Concurrently, *N. dombeyi* type started a rising trend that peaked between ~10,000 and 10,800 cal yr BP, following peak abundance of *Misodendron* and an abrupt increase of ~75% in Poaceae (252–257 cm) that led to a short-lived maximum at ~11,300 cal yr BP. Poaceae then declined gradually and achieved a fluctuating plateau centered at ~44%. We interpret the rapid increase in Poaceae as an immediate response of pioneer grasses that colonized the recently exposed lake bottom in the Pantano Dumestre site, while arboreal vegetation was increasing in site's vicinity. Our chronology indicates that the terrestrialization of the site and associated vegetation changes occurred within ~200 years (Fig. 9).

Interpretation of the *Galium* type rise between ~11,600 and 13,100 cal yr BP is complicated by the coarse pollen taxonomy of the Rubiaceae family and the fact that extant species occupy diverse

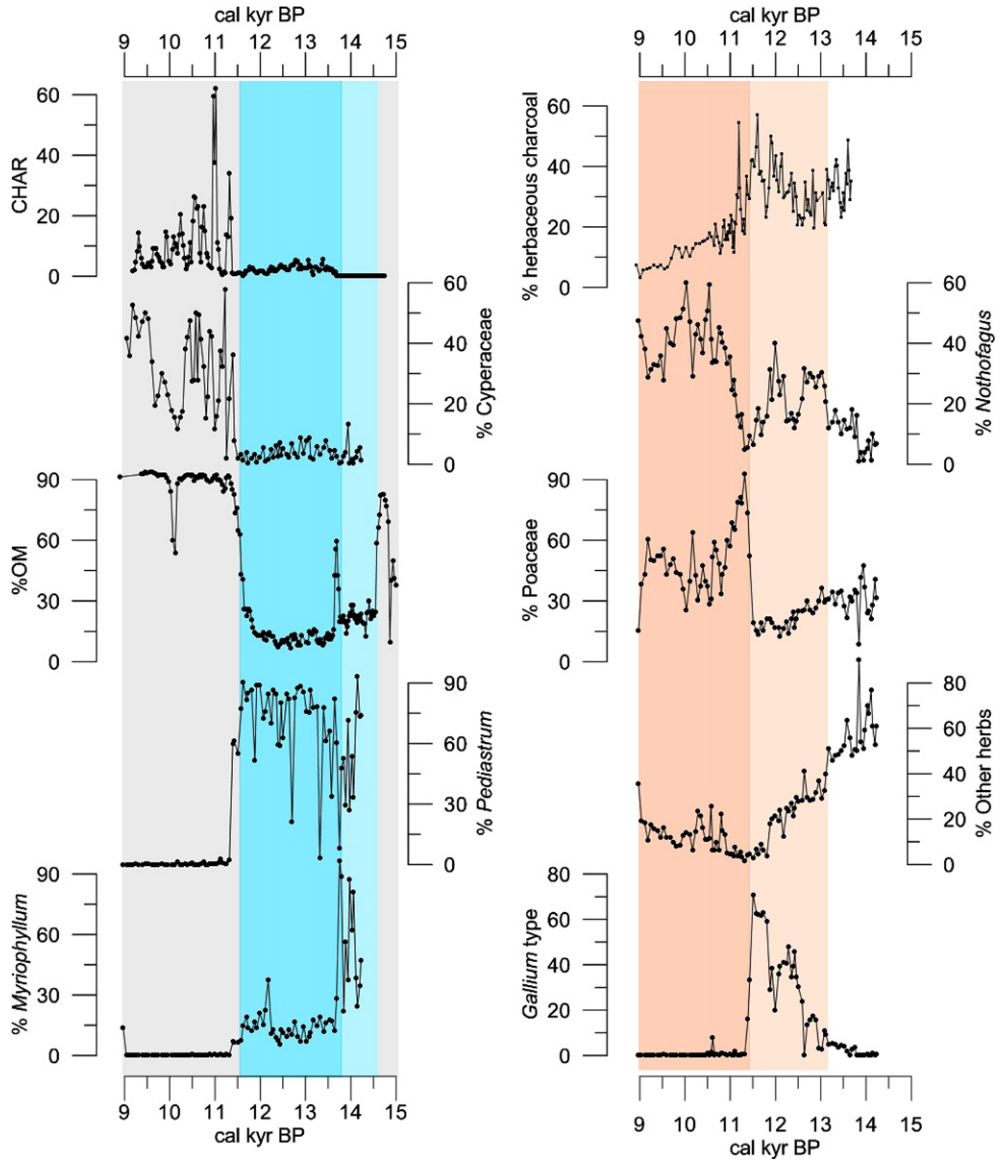

Fig. 9. Comparison of the loss-on-ignition data, charcoal analysis and palynology from core PS0607A. The gray vertical zones indicate times of peat deposition in the site, the light blue zone indicates a shallow lacustrine phase, the darker blue zone a deep lake phase, the light red zone denotes slight warming, the darker red zone substantial warming.

environments in southern Patagonia. We think the species *Galium magellanicum* is an adequate model to interpret the *Galium* type curve from Pantano Dumestre, considering its modern occurrence along river banks, lake shores, and moist meadows and from sea level up to 1200 m.a.s.l. (Roig et al., 1985). Fossil *Galium* type from Pantano Dumestre occurs in the context of lacustrine sedimentation characterized by horizontally lain silts with low organic content, high abundance of *Pediastrum*, increases of *N. dombeyi* type, a decline in cold-resistant herbs, and low abundance of *Myriophyllum*. We interpret the increase in *Galium* type between ~11,600 and 13,100 cal yr BP as the expansion of *G. magellanicum* in wetlands peripheral to Pantano Dumestre during the deep lake phase. The abrupt decline of *Galium* type at ~11,600 cal yr BP represents the disappearance of moist meadows surrounding the inundated Pantano Dumestre and the local establishment of Cyperaceae/*Sphagnum*-dominated bogs in the center of the basin.

The pollen record from Lago Eberhard also shows dominance of cold-resistant herbs (Poaceae, *Acaena*, Asteraceae subfamily Asteroidea) accompanied by lesser amounts of *N. dombeyi* type and Caryophyllaceae between ~12,800 and 11,600 cal yr BP (Fig. 10). We note that *Myriophyllum* reached its maximum abundance at the base of the record between ~12,600 and 12,800 cal yr BP and declined rapidly thereafter, suggesting an outward expansion of littoral environments triggered by deeper lake levels in Lago Eberhard (Fig. 10). Gradual increments in *N. dombeyi* type and *Blechnum* occurred between ~11,600 and 12,200 cal yr BP, followed by rapid increases in both taxa between ~11,400–11,600 and ~11,100–11,300
cal yr BP which alternate/follow centennial-scale increases in *Plantago* (Fig. 10). *N. dombeyi* type then achieved a high abundance plateau (~70%) between ~10,800 and 11,100 cal yr BP, suggesting closed-canopy Magellanic forests with a dense understory of ferns (Figs. 7 and 10). The organic and carbonate content of the lake cores co-vary with these fluctuations until ~11,200 cal yr BP, when the laminated authigenic calcite zone terminates abruptly and gives way to organic-rich gyttja that has persisted with little variation until the present (Figs. 3, 4 and 10). Unlike the Pantano Dumestre site, lacustrine sedimentation in Lago Eberhard has persisted until

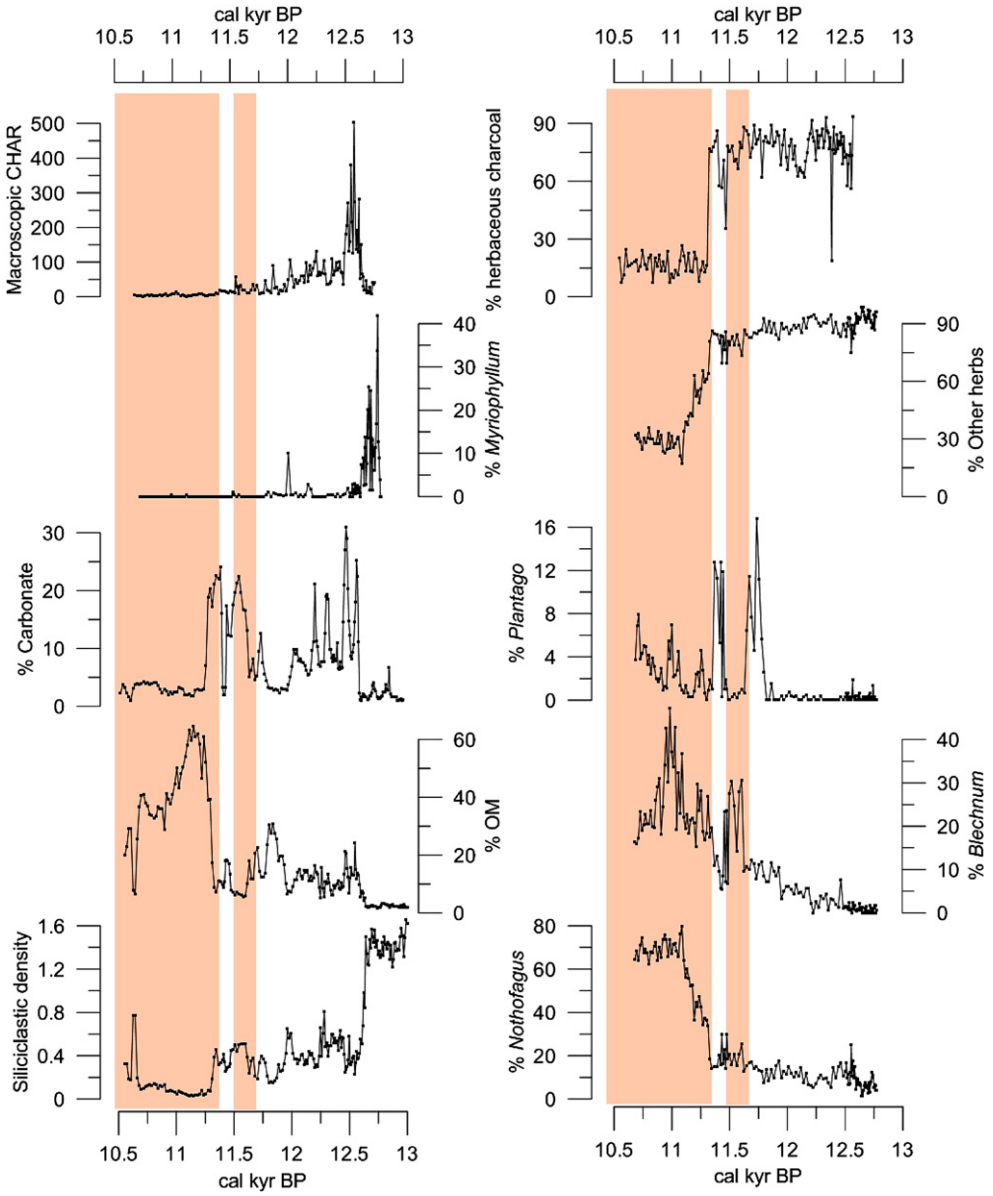

Fig. 10. Comparison of the loss-on-ignition data, charcoal analysis and palynology from core PS0401B. The red vertical zones indicate warm intervals.

the present. This important difference accounts for the abrupt increase in Poaceae and Cyperaceae in the Pantano Dumestre record at the beginning of the Holocene suggesting colonization of the newly exposed lake bottom by herbs and mosses. These results demonstrate that palynological records from bogs tend to depart from the regional signal by the influence of the vegetation that grows on them (Moreno et al., 2009a).

The macroscopic charcoal record from Pantano Dumestre reveals low charcoal abundance between ~11,400 and 13,700 cal yr BP, followed by an abrupt increase concurrent with the establishment of *Nothofagus* woodlands/scrublands around the site and terrestrialization of the Pantano Dumestre site at the beginning of the Holocene (Figs. 8 and 9). The percentage of herbaceous charcoal declined steadily from ~11,200 cal yr BP onward, coeval with an increase in woody fuels. Altogether, these data indicate a close correspondence between woodland/forest encroachment, a decline in herbaceous charcoal, increases in the magnitude and frequency of charcoal peaks, and terrestrialization of the lake, raising the possibility that a climate-induced shift in fire regimes could have acted as a catalyst of climate-induced vegetation changes during the Pleistocene–Holocene transition in the Pantano Dumestre record.

The macroscopic charcoal record from Lago Eberhard, on the other hand, shows peak fire activity between ~12,100 and 12,600 cal yr BP followed by a gradual and persistent decline in CHAR magnitude until ~10,400 cal yr BP (Figs. 8 and 10). The percentage of herbaceous charcoal in Lago Eberhard shows high values prior to ~11,300 cal yr BP, followed by an abrupt decline concurrent with rapid encroachment of *Nothofagus* forests/woodlands near Lago Eberhard. An important difference in local fire history is evident between sites, with Pantano Dumestre showing an increase in the frequency of high-magnitude charcoal peaks between ~10,000 and 11,600 cal yr BP whereas Lago Eberhard shows high frequency of low-magnitude but statistically significant charcoal peaks over the same interval. An inverse situation occurs around ~12,500 cal yr BP, when Pantano Dumestre shows frequent, low-magnitude and statistically significant charcoal peaks, while Lago Eberhard displays an increase in the frequency of

high-magnitude charcoal peaks. These results illustrate, on one hand, the spatial heterogeneity in fire occurrence between sites located ~30 km apart and less than 3 km from the modern coastline, and the fact that low-magnitude but statistically significant charcoal peaks provide a valuable source of information for understanding the evolution of fire regimes at a local scale. On the other hand, paleofire and paleovegetation histories derived from bog records tend to (over) emphasize a local signal, considering that azonal plant communities can thrive of their surface and that highly organic peat deposits can burn locally and impose a skewed signal that may depart from a regional fire history signal (Moreno et al., 2009a). Despite these differences we note that the frequency of local fires in both records shows a common pattern and chronology, with a decline between ~11,600 and 12,700 cal yr BP, an increase between ~10,900 and 11,600 cal yr BP, and a subsequent decline between ~10,500 and 10,900 cal yr BP. We explain this correspondence as a shift in fire regimes at the Pleistocene/Holocene boundary, a broad-scale phenomenon observed in southern South America (Whitlock et al., 2007) and other continents (Power et al., 2008). Our results indicate that, at a regional scale, this shift was caused by a warm pulse, decline in precipitation and concomitant vegetation change which, in combination, generated the necessary spatial/temporal continuity and seasonal desiccation of coarse, woody fuels at the beginning of the Holocene.

Archeological findings from Cueva del Medio (51°34′4.40″S, 72°36′25.29″W) and C. Lago Sofía 1 (51°32′3.19″S, 72°34′21.49″W), located ~4 and ~8 km from Lago Eberhard, respectively, bracket the earliest human occupations in the Última Esperanza area between ~11,000 and 13,500 cal yr BP (Borrero, 2009), coincident with the chronology of statistically significant charcoal peaks in the Pantano Dumestre and Lago Eberhard sites. This correspondence raises the possibility that humans could have provided the ignition source for fires in the lowlands of Última Esperanza during the last glacial–interglacial transition. Our results, however, suggest that the primary control on the time evolution of fire magnitude and frequency in this newly deglaciated sector of SW Patagonia was climate and vegetation change at millennial and sub-millennial time scales.

In summary, the pollen, charcoal, and lithostratigraphy from Pantano Dumestre and the Eberhard site indicate the following sequence of events during the last glacial termination: (1) glacial recession from a stabilized post-LGM position prior to ~16,400 cal yr BP; (2) development of an ice-dammed proglacial lake in areas <150 m.a.s.l. until ~12,800 cal yr BP; (3) a step-wise pattern of glaciolacustrine regressions with discrete pulses at ~15,350 and ~12,800 cal yr BP; (4) sub-aerial deposition of peat in Pantano Dumestre between ~14,600 and 15,380 cal yr BP; (5) a transgressive lake phase in Pantano Dumestre in pulses at ~14,600 and ~13,600 cal yr BP; (6) dominance of cold-resistant herbs between ~11,600 and 14,600 cal yr BP; (7) increases in *N. dombeyi* type, *Misodendron, Blechnum,* and *Galium* type between ~11,600 and 13,100 cal yr BP (at the expense of cold-resistant herbs and shrubs) with marked centennial-scale fluctuations and deposition of laminated authigenic calcite in Lago Eberhard; and (8) terrestrialization and substantial increase in local fires in Pantano Dumestre starting at ~11,600 cal yr BP, concurrent with a rapid spread of *Nothofagus* forests and woodlands.

4.3. Paleoclimate inferences

Past changes in hydrologic balance recorded by the Pantano Dumestre and Lago Eberhard sites afford valuable information for deciphering paleoclimate changes in southwestern Patagonia during the last glacial termination. Because local precipitation in western Patagonia is strongly and positively correlated with zonal wind speeds in the path of the SWW, we interpret positive anomalies in hydrologic balance in this region as reflecting enhanced westerly flow, and vice versa. Latitudinal shifts in the zone of maximum SWW influence can also induce positive anomalies in local precipitation, in the case of southwestern Patagonia this could be accomplished via a poleward shift in the modern zone of maximum precipitation of SWW origin (Moreno et al., 2010), or through an equatorward shift in the hypothetical case that the SWW were already displaced south of their modern maximum. It must be borne in mind, however, the potential impact of site-specific, non-climatic processes affecting past lake-level fluctuations, such as the infilling of the lake basins by sediments. The fact that the center and deepest part of Pantano Dumestre site exhibits transitions from shallow-lake deposits to sub-aerial peat deposits between ~14,600–14,900, ~13,600–13,700 and ~11,200–11,500 cal yr BP, suggests to us that the hydrologic balance of the closed-basin lake that occupied the Pantano Dumestre basin during the last glacial termination was highly dynamic, triggering repeated and reversible terrestrializations as the hydrologic balance crossed thresholds induced by variations in SWW influence at millennial timescales.

Our data suggest multi-millennial variations in hydrologic balance with positive anomalies between ~11,600–15,350 cal yr BP (lake development), followed by conditions similar to the modern (peatland development) since ~11,600 cal yr BP (Figs. 9 and 11). Within the ~11,600–15,350 cal yr BP interval we detect millennial-scale variability in hydrologic balance with pulses of lake level rise that commenced at ~14,600 and ~13,600 cal yr BP, followed by a rapid regression between ~11,500–11,800 cal yr BP, which we interpret as a steep decline in hydrologic balance. Consistent with these findings, the Lago Eberhard record shows peak abundance of *Myriophyllum* and macroscopic charcoal between ~12,600 and 12,800 cal yr BP followed by a steady decline until ~11,600 cal yr BP, suggesting a trend toward a deeper lake and positive hydrologic balance. The difference in timing for the disappearance of *Myriophyllum* from the deepest sectors of Pantano Dumestre and Lago Eberhard is related to the fact that Lago Eberhard became a closed-basin lake subsequent to Pantano Dumestre because glacial lake Puerto Consuelo lingered at lower elevations until ~12,800 cal yr BP. Our results imply that the accentuation of the transgressive lake phase that started at ~13,600 cal yr BP in Pantano Dumestre continued in the Lago Eberhard record until ~12,600 cal yr BP and, therefore, the culmination of the transgressive lake level trend was achieved between ~11,800 and 12,600 cal yr BP. In addition, authigenic calcite deposition in Lago Eberhard suggests intense evaporation over this time interval, implying strong desiccating winds during summer time and, thus, enhanced precipitation seasonality. In sum, we infer stronger SWW influence starting at ~14,600 cal yr BP, followed by an intensification that started at ~13,600 cal yr BP and culminated between ~11,800 and 12,600 cal yr BP; this was followed by a major decline in SWW influence commencing at ~11,800 cal yr BP (Figs. 9–11).

We observe peak IRD deposition in the Lago Eberhard cores between ~13,100 and 13,600 cal yr BP, contemporaneous with deepening of the closed-basin lake that occupied the Pantano Dumestre basin (Fig. 11). This correspondence suggests that the readvance of the Última Esperanza glacier lobe occurred during a cold interval with positive hydrologic balance in SW Patagonia, brought by enhanced SWW influence. An alternative interpretation for the deep lake phase in Pantano Dumestre involves a rise in the surface elevation of glacial lake Puerto Consuelo and flooding of the Pantano Dumestre basin driven by a readvance of the Última Esperanza glacier lobe between ~11,800 and 13,600 cal yr BP. We rule out this possibility considering that: (i) the well-sorted, horizontally lain silts with low organic content deposited in Pantano

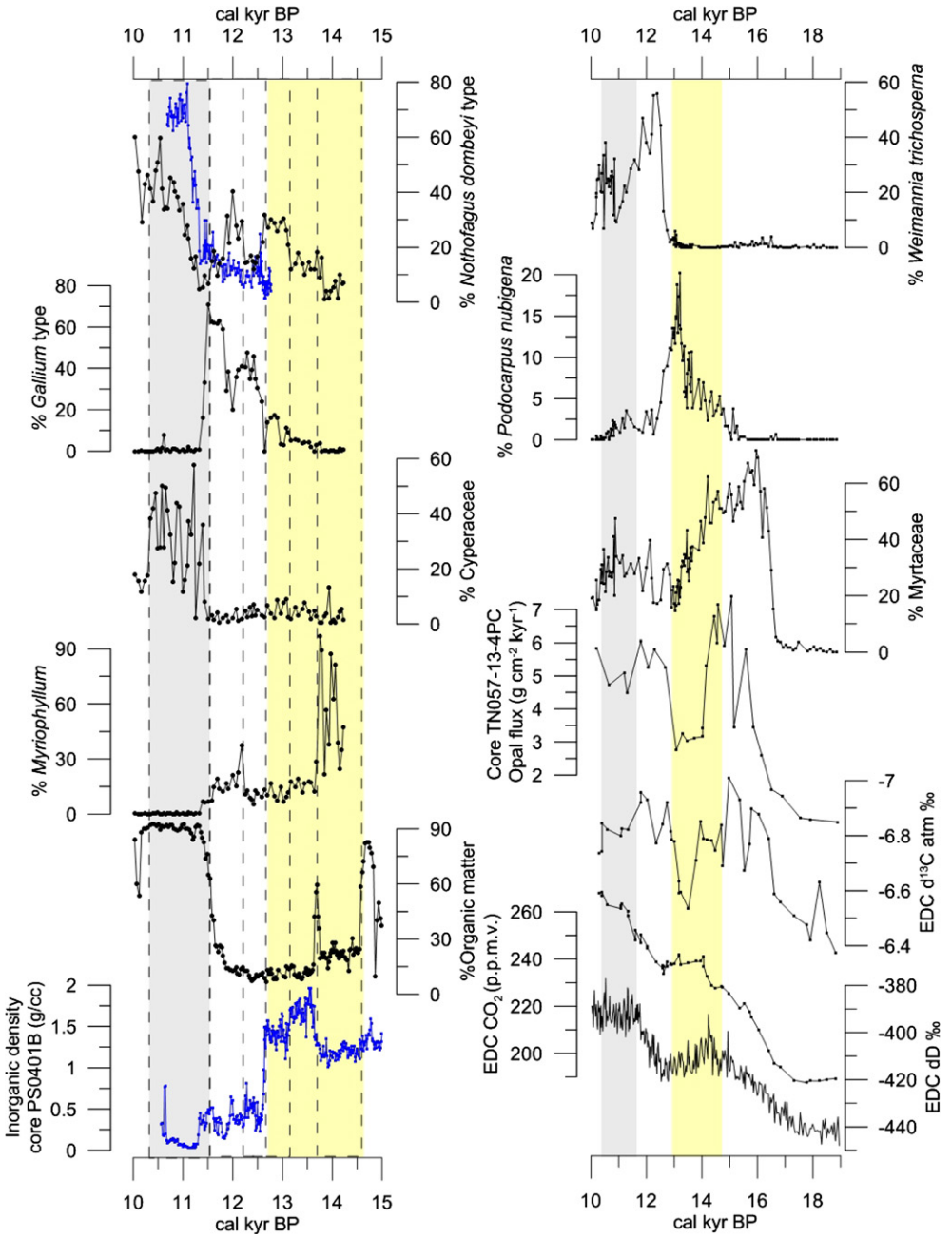

Fig. 11. Left panel: selected data from the Pantano Dumestre (black lines) and Lago Eberhard records (blue lines) presented in this paper. Right panel: palynological data (% *Weinmannia trichosperma*, % *Podocarpus nubigena*, % Myrtaceae) from NW Patagonia (Moreno and León, 2003), the opal flux record from core TN057-13-4PC (Anderson et al., 2009), the EDC records of atmospheric CO_2 concentration (Monnin et al., 2001), $\delta^{13}C$ of atmospheric CO_2 (Lourantou et al., 2010) and δD (Jouzel et al., 1987). The yellow vertical zone marks the timing of the Antarctic Cold Reversal, the gray zone indicates the earliest part of the Holocene, the intervening interval corresponds to the Younger Dryas chron. The dashed vertical lines mark the onset of major sub-millennial scale changes in the Pantano Dumestre and Lago Eberhard records. Although the left and right panel have different age scale lengths, the yellow and gray panels cover the same time intervals in each case.

Dumestre between ~12,800 and 13,600 cal yr BP lack clastic materials expected from flooding by a transgressive proglacial lake and subsequent IRD deposition of in the lake that occupied the Pantano Dumestre basin (Figs. 2 and 3), and (ii) the deep lake phase in Pantano Dumestre lasted until ~11,800 cal yr BP whereas glaciolacustrine sedimentation in the Eberhard site, located 10 m below Pantano Dumestre, ended at ~12,800 cal yr BP (Fig. 11). Therefore, flooding by glacial lake Puerto Consuelo is not a satisfactory explanation for the deep lake phase in Pantano Dumestre, suggesting that lake level changes fluctuations during this interval were driven primarily by changes in precipitation.

We interpret the palynological changes in Pantano Dumestre and Lago Eberhard as a rapid shift from a landscape dominated by cold-resistant alpine herbs between ~11,600 and 14,600 cal yr BP to *Nothofagus*-dominated forests/woodlands between ~10,000 and 11,600 cal yr BP, implying a treeline rise at ~11,600 cal yr BP. Interpretation of this vegetation change requires understanding the predominant controls on the elevation, distribution and composition of the modern plant communities occurring in the southern temperate Andes. A study on the spatial and temporal variation in *N. pumilio* growth at tree line along its latitudinal range (35°40′S–55°S) in the Chilean Andes (Lara et al., 2005), concluded

that temperature has a spatially larger control on tree growth than precipitation, and found that this influence is particularly significant in the temperate Andes (>40°S). These results suggest that low temperatures are the main limiting factor for the occurrence of woodlands and forests at high elevations in the Andes, considering that precipitation increases with elevation at any given latitude (Lara et al., 2005). Therefore, we conclude that the main driver for a treeline rise at ~11,600 cal yr BP was a warm event rather than a precipitation increase. Alternatively, our palynological results could be interpreted as a shift from an assemblage dominated by drought-resistant steppe herbs to moisture-demanding *Nothofagus*-dominated forests. One shortcoming of this alternative interpretation is that the observed transition in the upland vegetation was contemporaneous with an abrupt decline in hydrologic balance that drove the terrestrialization of Pantano Dumestre, suggesting that positive anomalies in precipitation prevailed prior to ~11,600 cal yr BP and yet arboreal vegetation was unable to expand and establish closed-canopy Magellanic forests in the lowlands of Última Esperanza (Fig. 11), even though the pollen records from Pantano Dumestre and Lago Eberhard suggest the local presence of *Nothofagus* (~20%) at that time (Fig. 11).

We conclude that the limiting factor for the establishment of arboreal vegetation under these humid conditions were low temperatures and strong winds. Within the predominantly cold-wet and windy interval between ~11,600 and 14,600 cal yr BP we detect slight warming beginning at ~13,100 cal yr BP with centennial-scale oscillations until ~11,600 cal yr BP. Our results suggest that the climatic transition from the Pleistocene into the Holocene in SW Patagonia involved rapid warming and a substantial decline in precipitation of SWW origin at ~11,600 cal yr BP, preceded by a highly variable warming trend between ~11,600 and 13,100 cal yr BP.

4.4. Regional implications

The majority of paleoecological studies that span the interval between ~10,000 and 15,000 cal yr BP from areas of southwestern Patagonia and Tierra del Fuego (50°–55°S) where the local precipitation is positively correlated with zonal SWW flow, reveal a common pattern: (1) overwhelming dominance of herbs/shrubs prior to ~11,500 cal yr BP, aspect that most authors have interpreted as representing a dry climate; (2) sub-millennial scale changes in herbs/shrubs between ~11,500 and 15,000 cal yr BP, which all authors have interpreted as representing moisture fluctuations; (3) moderate increases in *Nothofagus* between ~11,500 and 13,000 cal yr BP; followed by (4) large increases in *Nothofagus* and paleofires after ~11,500 cal yr BP, which most authors have interpreted as forest expansion in response to warmer, wetter conditions. Although our results from the Última Esperanza region are consistent with the palynostratigraphy described above, we detect important differences in the composition of the paleovegetation, the timing, frequency, magnitude, and direction of changes (attributable to geographic location, sampling resolution, depositional setting, and dating control), and the climatic interpretation of the assemblages (see Section 4.3).

Most of the previously published studies are based on cores collected from modern peatlands, sites that had already converted and remained as bogs through the ~11,500–15,000 cal yr BP period and, therefore, their inferences on hydrologic balance changes rely on the climatic interpretation of fossil pollen and charcoal records (Heusser, 1989a; Markgraf, 1993a, b; Heusser et al., 2000; McCulloch et al., 2000; McCulloch and Davies, 2001; Villa-Martínez and Moreno, 2007) and, in one case, on a comparison with a stable isotope record from fossil mosses from the same core (Markgraf and Huber, 2011). One difficulty with palynological records developed from bogs, however, is distinguishing local from extra-local and regional signals of past vegetation change which, in combination with the coarse taxonomic resolution and broad geographic and climatic distribution of the palynoflora from this region, pose important challenges for interpreting the extra-local vegetation and climate conditions (Moreno et al., 2009a). Previous studies from the westernmost sites along the Pacific coast of southwestern Patagonia (Gran Campo Nevado, Lago Tamar) (Fesq-Martin et al., 2004; Lamy et al., 2011), and Lago Guanaco in the Torres del Paine area (Moreno et al., 2010) offer the opportunity to examine changes in hydrologic balance through past variations in depositional environments (sub-aerial vs. subaquatic, littoral vs. profundal, precipitation of authigenic calcite, etc.). These studies provide an independent line of evidence for testing and refining the climatic inferences based on paleoecological data. We identify some outstanding similarities and differences between the latter studies and our results from the Última Esperanza region:

1. Pantano Dumestre, Lago Guanaco, Gran Campo Nevado and L. Tamar record lacustrine sedimentation in small closed-basin lakes between ~11,600 and 14,600 cal yr BP. Organic lacustrine sedimentation in L. Eberhard started later, at ~12,800 cal yr BP, in response to ice recession and lowering of glacial lake Puerto Consuelo below 70 m.a.s.l., leaving this basin exposed to sub-aerial conditions. Based on these data we interpret that positive hydrologic balance in southwestern Patagonia permitted the deposition of organic lake sediments in sites located on the eastern and western foothills of the Andes between ~11,600 and 14,600 cal yr BP.
2. Unlike the other sites, Pantano Dumestre shows sub-aerial accumulation of biogenic material in a peatland between ~14,600 and 14,900 cal yr BP, followed by a lacustrine phase as indicated by the lithostratigraphy and palynology discussed above. The implication of these findings is that the lacustrine phase represents a positive anomaly in hydrologic balance relative to the ~14,600–14,900 cal yr BP interval.
3. The lakes that occupied the Pantano Dumestre and Gran Campo Nevado basins underwent terrestrialization starting at ~11,800 and ~11,200 cal yr BP, respectively, suggesting that hydrologic balance in both cases turned negative and led to the disappearance of permanent water bodies during the Pleistocene–Holocene transition. An unconformity in the Lago Eberhard record between ~6600 and 10,600 cal yr BP indicates a low stand contemporaneous with terrestrialization of the lake's periphery, suggesting that: (i) a further decline in precipitation during the early Holocene was of sufficient magnitude to drive (temporarily) the hydrologic balance of this basin into negative values, and (ii) the uninterrupted accumulation of organic lake sediments with preservation of cm- to mm-scale authigenic calcite laminae in the lake cores between ~11,600 and 12,800 cal yr BP suggests a deep, permanent water body and positive hydrologic balance higher than the observed Holocene variations.
4. Lago Eberhard and L. Guanaco record precipitation of laminated authigenic calcite between ~11,600 and 12,800 and ~11,400–12,500 cal yr BP, respectively, revealing a contrast with the westernmost sites along the Pacific coast of southwestern Patagonia (L. Tamar and Gran Campo Nevado) and with Pantano Dumestre. The deposition of laminated authigenic calcite occurred during a time of positive hydrologic balance, colder conditions, and enhanced evaporation throughout the region. We note an apparent west to east contrast in which the easternmost lakes exhibit laminated calcite deposition between ~11,600 and 12,500 cal yr BP, in response to higher-than-present wind speeds and annual precipitation, and stronger-than-present evaporation seasonality at that time (Moreno et al., 2009b).

Geomorphic and stratigraphic studies in SW Patagonia and Tierra del Fuego have identified glacial readvances during the last glacial termination. Available chronologies from the Estrecho de Magallanes and Seno Skyring (Fig. 1) suggest that this event occurred sometime between the deposition of the R1 tephra (~14,800 cal yr BP according to Sagredo et al. (2011)) and 12,000 cal yr BP (Sugden et al., 2005; Kilian et al., 2007). A radiocarbon chronology from the Lago Argentino area (150 km north of the Última Esperanza region, Strelin et al., 2011) (Fig. 1), yielded ages of ~13,000 cal yr BP for the maximum glacier extent marked by the Puerto Banderas moraines. A study using cosmogenic dates on the same moraines by Ackert et al. (2008), however, gave ages of ~10,800 ± 500 cal yr BP. More recently, radiocarbon and cosmogenic glacial chronologies from Torres del Paine National Park, in combination with tephrochronology (Moreno et al., 2009b) (Fig. 1), constrained the age of a readvance of the Nordenskjöld and Paine ice lobes between ~12,600 and 14,800 cal yr BP. Our data from the Lago Eberhard cores suggest enhanced iceberg discharge and IRD delivery into glacial lake Puerto Consuelo, which together with the mapping and interpretation of Sagredo et al. (2011), indicate a readvance of the Seno Última Esperanza ice lobe between ~13,100 and 13,600 cal yr BP (Fig. 11). This was followed by lowering of the proglacial lake in response to glacial retreat and drainage of glacial lake Puerto Consuelo toward the Pacific Ocean (Figs. 3 and 4) (Sagredo et al., 2011). These results match the timing of glacial fluctuations from Torres del Paine National Park (Moreno et al., 2009b) and the radiocarbon chronology for the Puerto Bandera moraines (Strelin et al., 2011), suggesting that outlet glaciers from an expanded South Patagonian Ice Field readvanced over the course of the last glacial termination and attained maximum positions during the Antarctic Cold Reversal (dated between ~12,800 and 14,500 cal yr BP) (Jouzel et al., 2001). This was followed by glacial retreat and drainage of large ice-dammed proglacial lakes toward the Pacific during Younger Dryas time (dated between ~11,700 and 12,800 cal yr BP) (Rasmussen et al., 2006), though the pattern and rates of glacial recession are still poorly constrained.

By integrating the lithostratigraphy and palynology from the Pantano Dumestre and Lago Eberhard sites we interpret an extreme cold phase between ~13,100 and 14,600 cal yr BP, followed by slight and variable warming between ~11,600 and 13,100 cal yr BP, and a major warm phase between ~10,000 and 11,600 cal yr BP (Fig. 11). These changes occurred in the context of moisture variations attributable to changes in the amount of precipitation of westerly origin which, in this sector of Patagonia, is correlated with the zonal strength of the SWW. Our data suggest: (1) precipitation similar to the modern between ~14,600 and 14,900 cal yr BP, followed by (2) an increase between ~13,600 and 14,600 cal yr BP (positive anomalies in SWW influence), (3) an accentuation of that increase at ~13,600 cal yr BP that led to a maximum in precipitation and wind-driven seasonal evaporation between ~11,600 and 12,600 cal yr BP, and (4) a major decline in precipitation between ~10,000 and 11,600 cal yr BP (negative anomalies in SWW influence).

Studies from small closed-basin lakes in northwestern (40°–42°S) and Central Patagonia (47°S), sectors where local precipitation is also positively and strongly correlated with zonal SWW flow, indicate (Moreno et al., 1999; Moreno and León, 2003; Moreno, 2004; Villa-Martínez et al., 2012): (1) closed-canopy North Patagonian rainforests dominated by thermophilous trees (peak abundance of Myrtaceae in Fig. 11) between ~14,400 and 15,700 cal yr BP, interpreted as temperate-humid conditions; followed by (2) expansion of cold-resistant North Patagonian conifers starting at ~14,400 cal yr BP (*Podocarpus nubigena* in Fig. 11) indicative of cooler, wetter conditions, and (3) a decline but persistence of cold-resistant conifers, a rise in littoral chironomids (Massaferro et al., 2009), abrupt increases of North Patagonian trees favored by disturbance (*Weinmannia trichosperma* in Fig. 11), and intense fire activity between ~11,500 and 12,800 cal yr BP. Moreno and León (2003) and Massaferro et al. (2009) interpreted the latter changes as a decline in precipitation under cool-temperate conditions. The Lago Augusta site, located on the eastern slopes of the Central Patagonian Andes (47°S), shows increases in the cold-resistant hygrophilous conifers *P. nubigena* and *Pilgerodendron uviferum*, which Villa-Martínez et al. (2012) interpreted as an increase in precipitation under cool-temperate conditions between ~11,800 and 13,400 cal yr BP. Thus, northwestern and central Patagonian sites record (4) disappearance of cold-resistant conifers at ~11,500 cal yr BP, diversification of the forest assemblage and increases in species with broad tolerance and ample distributions in climatic and geographic space, along with increased fire activity and terrestrialization of several sites, thus marking the onset of warm/dry conditions at the beginning of the Holocene.

In the context of the last 15,000 years, Moreno (2004) interpreted positive anomalies in precipitation and stronger SWW flow in northwestern Patagonia (~41°S) between ~11,500 and 14,400 cal yr BP. This was followed by a conspicuous decline toward "zero anomalies" (average conditions) between ~11,000 and 12,800 cal yr BP and strongly negative anomalies between ~9000 and 11,500 cal yr BP. We note a correspondence in timing between positive anomalies in hydrologic balance prior to ~11,600 cal yr BP, followed by negative anomalies during the Holocene. Within the positive anomaly interval at the end of the Pleistocene we identify an early phase before ~12,700 cal yr BP in northwestern and southwestern Patagonia with strong positive anomalies, followed by a decline toward average conditions in northwestern Patagonia coeval with a further increase toward peak positive anomalies in southwestern Patagonia. The temporal and geographic distribution of precipitation anomalies can be used to reconstruct variations in the strength and latitudinal position of the SWW. We expect that persistent shifts in the latitudinal position of the SWW (equator- or poleward) at multi-millennial timescales should result in synchronous precipitation anomalies of opposite sign in the studied regions (a northward shift would feature positive anomalies in northwestern Patagonia and negative anomalies in southwestern Patagonia, and viceversa), whereas changes in the strength of zonal flow should result in simultaneous anomalies of the same sign (synchronous positive anomalies would indicate stronger SWW, and viceversa). We recognize the following patterns: (1) an average behavior of the SWW between ~14,600 and 15,700 cal yr BP, (2) symmetrically enhanced SWW influence in northwestern and southwestern Patagonia between ~12,700 and 14,600 cal yr BP, (3) asymmetric changes in SWW influence between ~11,500 and 12,600 cal yr BP with a decline in northwestern and a rise in southwestern Patagonia, and (4) symmetrically reduced SWW influence in northwestern and southwestern Patagonia between ~10,000 and 11,500 cal yr BP. These patterns suggest that the SWW behaved in a manner similar to the modern between ~14,600 and 15,700 cal yr BP, became stronger between ~12,700 and 14,600 cal yr BP, shifted poleward between ~11,000 and 12,600 cal yr BP, and then weakened between ~10,000 and 11,000 cal yr BP.

4.5. Hemispheric and global implications

Our reconstruction of SWW activity allows assessment of the role of the SWW- Southern Ocean (SO) coupled system as a driver of past variations in atmospheric CO_2 during the last glacial termination. Fig. 11 shows a summary of our results compared with Antarctic ice core data (Monnin et al., 2001; Jouzel et al., 2007;

Lourantou et al., 2010), opal flux in the Atlantic sector of the SO (interpreted as a proxy for wind-induced upwelling, Anderson et al., 2009), and selected palynological taxa from the Huelmo site in NW Patagonia (Moreno and León, 2003).

We note that sub-aerial accumulation of peat in Pantano Dumestre (illustrated by peak percent of organic matter) between 14,600 and 14,900 cal yr BP was contemporaneous with peak abundance of Myrtaceae in Huelmo, indicating cool-temperate conditions and precipitation regimes similar to the modern in northwestern and southwestern Patagonia. This was contemporaneous with maximum values in Antarctic temperatures, atmospheric CO_2 concentration in the EPICA Dome Concordia ice core (EDC) (Monnin et al., 2001), the opal flux record from core TN057-13-4PC obtained from the Atlantic sector of the SO (Anderson et al., 2009) (Fig. 11). At the same time, the $\delta^{13}C$ CO_2 record from EDC (interpreted as intense degassing of CO_2-enriched deep waters in the SO) (Lourantou et al., 2010) attained low and variable values. Together, these results indicate that the SWW exerted their influence along a broad latitudinal range, encompassing northwestern and southwestern Patagonia and the SO, and drove degassing of CO_2-rich deep waters via enhanced wind-driven upwelling in the SO.

A lake transgressive trend started in Pantano Dumestre at ~14,600 cal yr BP (illustrated by a decline in % organic matter) which later intensified at ~13,600 cal yr BP (rapid decline in *Myriophyllum*), concurrent with glacial readvances of the Última Esperanza glacier lobe (enhanced IRD deposition in Lago Eberhard, illustrated by the culmination of a prominent rise in inorganic density of core PS0401B, Fig. 11), the Río Paine and Nordenskjold ice lobes in Torres del Paine National Park and deposition of the Puerto Banderas moraines in Lago Argentino (Moreno et al., 2009b; Strelin et al., 2011). This was contemporaneous with a reversal to cooler/wetter conditions in northwestern Patagonia (decline in Myrtaceae and increased *P. nubigena* in the Huelmo record) starting at ~14,400 cal yr BP, along with high-latitude cooling, a halt in the deglacial atmospheric CO_2 rise during the Antarctic Cold Reversal (ACR), and reversals in the $\delta^{13}C$ CO_2 from the EDC and the opal flux record from core TN057-13-4PC (Fig. 11), interpreted as reduced diatom productivity and a decline in upwelling of deep old waters in the SO (Anderson et al., 2009; Lourantou et al., 2010). Together, these results indicate stronger SWW flow in northwestern and southwestern Patagonia and diminished influence in the SO, implying a northward shift of the southern westerly margin that attenuated degassing of CO_2-rich deep waters via diminished wind-driven upwelling in the SO.

Increases in *Galium* type and *N. dombeyi* type in Pantano Dumestre starting at ~12,800–13,100 cal yr BP mark the onset of slightly warmer conditions (cold, but less severe than during the ACR) (Figs. 10 and 11), concurrent with deepening of Lago Eberhard, lowering of glacial lake Puerto Consuelo as glacial recession in the Andes triggered its drainage toward the Pacific (Sagredo et al., 2011). At the same time Patagonian glaciers abandoned their ACR maximum positions (Moreno et al., 2009b; Strelin et al., 2011), pollen records from northwestern Patagonian show intense fire activity and disturbance in the vegetation (rise in *Weinmannia trichosperma*, decline in all other trees), Antarctic ice cores show the onset of a warming trend and resumption of the deglacial rise in atmospheric CO_2, the opal flux record from the SO shows an increasing trend, and the $\delta^{13}C$ CO_2 record shows a sustained excursion toward negative values (Fig. 11). These conditions persisted until ~11,500 cal yr BP as a reversal in high-latitude marine and ice core records and a shift toward opposite combinations of temperature and precipitation conditions in northwestern and southwestern Patagonia during Younger Dryas time (Fig. 11). Collectively, these results indicate diminished SWW influence in northwestern Patagonia and stronger SWW flow in southwestern Patagonia and the SO, suggesting a southward shift of the SWW that triggered intense degassing of CO_2-rich deep waters via enhanced wind-driven upwelling in the SO. We interpret glacial recession in southwestern Patagonia and modest increases in relatively thermophilous taxa in our pollen records from Última Esperanza as a response to slight warming driven by rapid increases in atmospheric greenhouse gases (CO_2, CH_4).

We observe terrestrialization of lakes between ~10,000 and 11,500 cal yr BP and broad-scale increases in fire activity in northwestern and southwestern Patagonia, forest/woodland expansion in SW Patagonia and disappearance of cold-resistant conifers in northwestern Patagonia, the warmest millennia recorded during the last glacial cycle in Antarctic ice cores, persistence of high atmospheric CO_2 concentrations, high opal flux in the SO and a shift toward negative $\delta^{13}C$ CO_2 values (Fig. 11). We interpret the mid-latitude records as indicative of abrupt warming and decline in precipitation at ~11,500 cal yr BP, followed by a widespread decline in precipitation that Moreno et al. (2010) interpreted as a multi-millennial scale weakening of the SWW between ~7800 and 10,600 cal yr BP. A recent synthesis of paleoclimate records sensitive to past changes in the SWW (Fletcher and Moreno, 2011a, b) recognized a similar pattern in other southern mid-latitude landmasses. This led to the conclusion that the SWW changed in a zonally symmetric manner at multi-millennial timescales during the last 14,000 years, with a minimum in SWW strength between ~7000 and 10,000 cal yr BP. The latter correlates with a conspicuous decline in atmospheric CO_2 concentration in Antarctic ice cores over the same interval, suggesting a strong linkage between SWW intensity and degassing of the deep ocean via wind-induced upwelling in the SO (Moreno et al., 2010; Fletcher and Moreno, 2011a, b) (Fig. 11).

The records from Pantano Dumestre and Lago Eberhard indicate a major climate transition at 11,600 cal yr BP that matches the recently redefined Pleistocene–Holocene boundary at 11,700 cal yr BP on the basis of the NGRIP ice core (Walker et al., 2009). Our results suggest a synchronous inter-hemispheric climate response for this major transition, which contrasts with the out-of-phase or antiphased pattern evident in the millennial-scale paleoclimate events during the last glacial termination, the LGM, and marine isotope stage 3.

5. Conclusions

- The Última Esperanza ice lobe retreated from a stabilized post-LGM position prior to ~16,400 cal yr BP and led to the development of an ice-dammed proglacial lake (glacial lake Puerto Consuelo) in sectors below 150 m.a.s.l.
- This was followed by a step-wise pattern of glaciolacustrine regressions with discrete pulses at ~15,350 and ~12,800 cal yr BP (establishment of small closed-basin lakes in the Pantano Dumestre and Eberhard sites, respectively).
- A regressive lake level trend in Pantano Dumestre led to the sub-aerial deposition of peat between ~14,600 and 14,900 cal yr BP, suggesting negative hydrologic balance brought by a decline in precipitation.
- A transgressive lake phase occurred in Pantano Dumestre with pulses at ~14,600 and ~13,600 cal yr BP and led to the development of a closed-basin lake. The fact that littoral macrophytes disappeared from the Lago Eberhard record between 11,600 and 12,600 cal yr BP suggests to us deepening of the lake in response to the same transgressive lake phase recorded in Pantano Dumestre. We conclude that Pantano Dumestre and Lago Eberhard were at their deepest between 11,600 and 12,600 cal yr BP. We interpret these pulses as

increases in precipitation brought by intensification of the SWW throughout Patagonia between ~12,600 and 14,600 cal yr BP and a poleward shift between ~11,600 and 12,600 cal yr BP.

- Cold-resistant herbs dominated the pollen records between ~11,600 and 14,600 cal yr BP.
- We detect a rise in *N. dombeyi* type, *Misodendron, Blechnum,* and *Galium* type between ~11,600 and 13,100 cal yr BP along with marked centennial-scale fluctuations in the Pantano Dumestre site while laminated authigenic calcite were deposited in Lago Eberhard. We interpret these results as indicating slight warming under predominantly cold, wet, and windy conditions.
- Terrestrialization and increase in local fires in Pantano Dumestre started at ~11,600 cal yr BP, concurrent with a rapid spread of *Nothofagus* forests/woodlands in Pantano Dumestre and Lago Eberhard. We interpret these results as indicating substantial warming and a decline in precipitation brought by weaker SWW throughout Patagonia starting at ~11,600 cal yr BP. The fact that precipitation regimes were much higher prior to ~11,600 cal yr BP implies that low temperatures and high wind speeds were the primary factor inhibiting arboreal expansion in this sector of SW Patagonia at the end of the last glaciation.
- The geographic distribution of precipitation anomalies throughout western Patagonia suggest that the SWW strengthened during the ACR, shifted poleward during the YD, and became weaker at the beginning of the Holocene. Covariation in upwelling strength and atmospheric CO_2 strongly suggest that changes in the SWW–SO coupled system were a primary factor governing CO_2 fluxes from the deep ocean to the atmosphere during the last glacial termination.

Acknowledgments

This research was funded by Fondecyt grants 1040204, 1070991, 1110612, ICM grant P02-51, and PFB-23 from Conicyt. We thank C.M. Moy and T. Guilderson for their contribution to the development of the radiocarbon chronology, C.R. Stern for the analysis of tephras, D. Ariztegui for analyzing the laminated carbonates from Lago Eberhard, and L. Hernández for sampling, processing the palynological samples from Pantano Eberhard and conducting macroscopic charcoal analysis of Pantano Dumestre. Our appreciation goes to J.P. Francois, J.C. Moreno, R. Flores, A. Prieto, and M. San Román for providing field support. We thank R. Eberhard for permission to work and collect samples from Estancia Puerto Consuelo, Myriam Pastene (Clínica Bellolio) for allowing access to digital X radiographs, and M. San Román from Universidad de Magallanes for logistic support at Campus Puerto Natales.

References

Ackert, R.P., Becker, R.A., Singer, B.S., Kurz, M.D., Caffee, M.W., Mickelson, D.M., 2008. Patagonian glacier response during the late glacial-Holocene transition. Science 321, 392–395.

Anderson, R.F., Ali, S., Bradtmiller, L.I., Nielsen, S.H.H., Fleisher, M.Q., Anderson, B.E., Burckle, L.H., 2009. Wind-driven upwelling in the Southern Ocean and the deglacial rise in atmospheric CO_2. Science 323, 1443–1448.

Anselmetti, F.S., Ariztegui, D., De Batist, M., Gebhardt, A.C., Haberzettl, T., Niessen, F., Ohlendorf, C., Zolitschka, B., 2009. Environmental history of southern Patagonia unravelled by the seismic stratigraphy of Laguna Potrok Aike. Sedimentology 56, 873–892.

Bengtsson, L., Enell, M., 1986. Chemical analysis. In: Berglund, B.E. (Ed.), Handbook of Palaeoecology and Palaeohydrology. John Wiley & Sons, pp. 423–451.

Borrero, L.A., 2009. The elusive evidence: the archeological record of the South American extinct megafauna. In: Haynes, G. (Ed.), American Megafaunal Extinctions at the End of the Pleistocene. Springer, Netherlands, pp. 145–168.

Denton, G.H., Anderson, R.F., Toggweiler, J.R., Edwards, R.L., Schaefer, J.M., Putnam, A.E., 2010. The last glacial termination. Science 328, 1652–1656.

Faegri, K., Iversen, J., 1989. Textbook of Pollen Analysis. John Wiley & Sons.

Fesq-Martin, M., Friedmann, A., Peters, M., Behrmann, J., Kilian, R., 2004. Late-glacial and Holocene vegetation history of the Magellanic rain forest in southwestern Patagonia, Chile. Vegetation History and Archaeobotany 13, 249–255.

Fletcher, M.-S., Moreno, P.I., 2011a. Have the Southern Westerlies changed in a zonally symmetric manner over the last 14,000 years? A hemisphere-wide take on a controversial problem. Quaternary International.

Fletcher, M.-S., Moreno, P.I., 2011b. Zonally symmetric changes in the strength and position of the Southern Westerlies drove atmospheric CO_2 variations over the past 14 k.y. Geology 39, 419–422.

Garreaud, R.D., 2007. Precipitation and circulation covariability in the extratropics. Journal of Climate 20, 4789–4797.

Haberzettl, T., Corbella, H., Fey, M., Janssen, S., Lucke, A., Mayr, C., Ohlendorf, C., Schdbitz, F., Schleser, G.H., Wille, M., Wulf, S., Zolitschka, B., 2007. Lateglacial and Holocene wet-dry cycles in southern Patagonia: chronology, sedimentology and geochemistry of a lacustrine record from Laguna Potrok Aike, Argentina. Holocene 17, 297–310.

Heiri, O., Lotter, A.F., Lemcke, G., 2001. Loss on ignition as a method for estimating organic and carbonate content in sediments: reproducibility and comparability of results. Journal of Paleolimnology 25, 101–110.

Heusser, C.J., 1989a. Late Quaternary vegetation and climate of Southern Tierra Del Fuego. Quaternary Research 31, 396–406.

Heusser, C.J., 1989b. Southern westerlies during the last glacial maximum. Quaternary Research 31, 423–425.

Heusser, C.J., Heusser, L.E., Lowell, T.V., Moreira, A., Moreira, S., 2000. Deglacial palaeoclimate at Puerto del Hambre, subantarctic Patagonia, Chile. Journal of Quaternary Science 15, 101–114.

Higuera, P.E., Brubaker, L.B., Anderson, P.M., Hu, F.S., Brown, T.A., 2009. Vegetation mediated the impacts of postglacial climate change on fire regimes in the south-central Brooks Range, Alaska. Ecological Monographs 79, 201–219.

Imbrie, J., Boyle, E.A., Clemens, S.C., Duffy, A., Howard, W.R., Kukla, G., Kutzbach, J., Martinson, D.G., McIntyre, A., Mix, A.C., Molfino, B., Morley, J.J., Peterson, L.C., Pisias, N.G., Prell, W.L., Raymo, M.E., Schackleton, N.J., Toggweiler, J.R., 1992. On the structure and origin of major glaciation cycles 1. Linear responses to Milankovitch forcing. Paleoceanography 7, 701–738.

Jouzel, J., Lorius, C., Petit, J.R., Genthon, C., Barkov, N.I., Kotlyakov, V.M., Petrov, V.M., 1987. Vostok ice core: a continuous isotope temperature record over the last climatic cycle (160,000 years). Nature 329, 403–408.

Jouzel, J., Masson-Delmotte, V., Cattani, O., Dreyfus, G., Falourd, S., Hoffmann, G., Minster, B., Nouet, J., Barnola, J.M., Chappellaz, J., Fischer, H., Gallet, J.C., Johnsen, S., Leuenberger, M., Loulergue, L., Luethi, D., Oerter, H., Parrenin, F., Raisbeck, G., Raynaud, D., Schilt, A., Schwander, J., Selmo, E., Souchez, R., Spahni, R., Stauffer, B., Steffensen, J.P., Stenni, B., Stocker, T.F., Tison, J.L., Werner, M., Wolff, E.W., 2007. Orbital and millennial Antarctic climate variability over the past 800,000 years. Science 317, 793–796.

Jouzel, J., Masson, V., Cattani, O., Falourd, S., Stievenard, M., Stenni, B., Longinelli, A., Johnsen, S.J., Steffenssen, J.P., Petit, J.R., Schwander, J., Souchez, R., Barkov, N.I., 2001. A new 27 kyr high resolution East Antarctic climate record. Geophysical Research Letters 28, 3199–3202.

Kilian, R., Schneider, C., Koch, J., Fesq-Martin, M., Biester, H., Casassa, G., Arevalo, M., Wendt, G., Baeza, O., Behrmann, J., 2007. Palaeoecological constraints on late Glacial and Holocene ice retreat in the Southern Andes (53 degrees S). Global and Planetary Change 59, 49–66.

Lamy, F., Kilian, R., Arz, H.W., Francois, J.P., Kaiser, J., Prange, M., Steinke, T., 2011. Holocene changes in the position and intensity of the southern westerly wind belt. Nature Geoscience 3, 695–699.

Lara, A., Aravena, J.C., Villalba, R., Wolodarsky-Franke, A., Luckman, B., Wilson, R., 2001. Dendroclimatology of high-elevation *Nothofagus pumilio* forests at their northern distribution limit in the central Andes of Chile. Canadian Journal of Forest Research-Revue Canadienne De Recherche Forestiere 31, 925–936.

Lara, A., Villalba, R., Wolodarsky-Franke, A., Aravena, J.C., Luckman, B.H., Cuq, E., 2005. Spatial and temporal variation in *Nothofagus pumilio* growth at tree line along its latitudinal range (35 degrees 40′–55 degrees S) in the Chilean Andes. Journal of Biogeography 32, 879–893.

Lourantou, A., Lavric, J.V., Kohler, P., Barnola, J.M., Paillard, D., Michel, E., Raynaud, D., Chappellaz, J., 2010. Constraint of the CO_2 rise by new atmospheric carbon isotopic measurements during the last deglaciation. Global Biogeochemical Cycles 24.

Markgraf, V., 1989. Reply to Heusser's "Southern Westerlies during the Last Glacial Maximum". Quaternary Research 31, 426–432.

Markgraf, V., 1993a. Paleoenvironments and paleoclimates in Tierra-Del-Fuego and Southernmost Patagonia, South-America. Palaeogeography, Palaeoclimatology, Palaeoecology 102, 53–68.

Markgraf, V., 1993b. Younger Dryas in Southernmost South-America – an update. Quaternary Science Reviews 12, 351–355.

Markgraf, V., Huber, U.M., 2011. Late and postglacial vegetation and fire history in Southern Patagonia and Tierra del Fuego. Palaeogeography, Palaeoclimatology, Palaeoecology 297, 351–366.

Massaferro, J.I., Moreno, P.I., Denton, G.H., Vandergoes, M., Dieffenbacher-Krall, A., 2009. Chironomid and pollen evidence for climate fluctuations during the Last Glacial Termination in NW Patagonia. Quaternary Science Reviews 28, 517–525.

McCulloch, R.D., Bentley, M.J., Purves, R.S., Hulton, N.R.J., Sugden, D.E., Clapperton, C.M., 2000. Climatic inferences from glacial and palaeoecological evidence at the last glacial termination, southern South America. Journal of Quaternary Science 15, 409–417.

McCulloch, R.D., Davies, S.J., 2001. Late-glacial and Holocene palaeoenvironmental change in the central Strait of Magellan, southern Patagonia. Palaeogeography, Palaeoclimatology, Palaeoecology 173, 143–173.

Monnin, E., Indermuhle, A., Dallenbach, A., Fluckiger, J., Stauffer, B., Stocker, T.F., Raynaud, D., Barnola, J.M., 2001. Atmospheric CO_2 concentrations over the last glacial termination. Science 291, 112–114.

Moreno, P.I., 2004. Millennial-scale climate variability in northwest Patagonia over the last 15000 yr. Journal of Quaternary Science 19, 35–47.

Moreno, P.I., Francois, J.P., Villa-Martínez, R., Moy, C.M., 2009a. Millennial-scale variability in Southern Hemisphere westerly wind activity over the last 5000 years in SW Patagonia. Quaternary Science Reviews 28, 25–38.

Moreno, P.I., Francois, J.P., Villa-Martínez, R., Moy, C.M., 2010. Covariability of the Southern Westerlies and atmospheric CO_2 during the Holocene. Geology 39, 727–730.

Moreno, P.I., Kaplan, M.R., François, J.P., Villa-Martínez, R., Moy, C.M., Stern, C.R., Kubik, P.W., 2009b. Renewed glacial activity during the Antarctic Cold Reversal and persistence of cold conditions until 11.5 ka in SW Patagonia. Geology 37, 375–378.

Moreno, P.I., León, A.L., 2003. Abrupt vegetation changes during the last glacial to Holocene transition in mid-latitude South America. Journal of Quaternary Science 18, 787–800.

Moreno, P.I., Lowell, T.V., Jacobson, G.L., Denton, G.H., 1999. Abrupt vegetation and climate changes during the last glacial maximum and last termination in the Chilean Lake District: a case study from Canal de la Puntilla (41 degrees s). Geografiska Annaler Series A-Physical Geography 81A, 285–311.

Moy, C.M., Dunbar, R.B., Moreno, P.I., Francois, J.P., Villa-Martínez, R., Mucciarone, D.M., Guilderson, T.P., Garreaud, R.D., 2008. Isotopic evidence for hydrologic change related to the westerlies in SW Patagonia, Chile, during the last millennium. Quaternary Science Reviews 27, 1335–1349.

Power, M., Marlon, J., Ortiz, N., Bartlein, P., Harrison, S., Mayle, F., Ballouche, A., Bradshaw, R., Carcaillet, C., Cordova, C., Mooney, S., Moreno, P., Prentice, I., Thonicke, K., Tinner, W., Whitlock, C., Zhang, Y., Zhao, Y., Ali, A., Anderson, R., Beer, R., Behling, H., Briles, C., Brown, K., Brunelle, A., Bush, M., Camill, P., Chu, G., Clark, J., Colombaroli, D., Connor, S., Daniau, A.L., Daniau, A.L., Daniels, M., Dodson, J., Doughty, E., Edwards, M., Finsinger, W., Foster, D., Frechette, J., Gaillard, M.J., Gavin, D., Gobet, E., Haberle, S., Hallett, D., Higuera, P., Hope, G., Horn, S., Inoue, J., Kaltenrieder, P., Kennedy, L., Kong, Z., Larsen, C., Long, C., Lynch, J., Lynch, E., McGlone, M., Meeks, S., Mensing, S., Meyer, G., Minckley, T., Mohr, J., Nelson, D., New, J., Newnham, R., Noti, R., Oswald, W., Pierce, J., Richard, P., Rowe, C., Sanchez Goñi, M., Shuman, B., Takahara, H., Toney, J., Turney, C., Urrego-Sanchez, D., Umbanhowar, C., Vandergoes, M., Vanniere, B., Vescovi, E., Walsh, M., Wang, X., Williams, N., Wilmshurst, J., Zhang, J., 2008. Changes in fire regimes since the Last Glacial Maximum: an assessment based on a global synthesis and analysis of charcoal data. Climate Dynamics 30, 887–907.

Rasmussen, S.O., Andersen, K.K., Svensson, A.M., Steffensen, J.P., Vinther, B.M., Clausen, H.B., Siggaard-Andersen, M.L., Johnsen, S.J., Larsen, L.B., Dahl-Jensen, D., Bigler, M., Rothlisberger, R., Fischer, H., Goto-Azuma, K., Hansson, M.E., Ruth, U., 2006. A new Greenland ice core chronology for the last glacial termination. Journal of Geophysical Research-Atmospheres 111.

R Development Core Team, 2010. R: A Language and Environment for Statistical Computing. R Foundation for Statistical Computing, Vienna, Austria.

Reimer, P.J., Baillie, M.G.L., Bard, E., Bayliss, A., Beck, J.W., Blackwell, P.G., Ramsey, C.B., Buck, C.E., Burr, G.S., Edwards, R.L., Friedrich, M., Grootes, P.M., Guilderson, T.P., Hajdas, I., Heaton, T.J., Hogg, A.G., Hughen, K.A., Kaiser, K.F., Kromer, B., McCormac, F.G., Manning, S.W., Reimer, R.W., Richards, D.A., Southon, J.R., Talamo, S., Turney, C.S.M., van der Plicht, J., Weyhenmeye, C.E., 2009. Intcal09 and Marine09 radiocarbon age calibration curves, 0–50,000 years cal BP. Radiocarbon 51, 1111–1150.

Roig, F.A., Anchorena, J., Dollenz, O., Faggi, A.M., Mendez, E., 1985. Las comunidades vegetales de la Transecta Botánica de la Patagonia Austral. Primera parte: la vegetación del área continental. In: Boelcke, O., Moore, D.M., Roig, F.A. (Eds.), Transecta Botánica de la Patagonia Austral. Consejo Nacional de Investigaciones Científicas y Técnicas, Buenos Aires, Argentina, p. 733.

Rojas, M., Moreno, P., Kageyama, M., Crucifix, M., Hewitt, C., Abe-Ouchi, A., Ohgaito, R., Brady, E.C., Hope, P., 2009. The Southern Westerlies during the last glacial maximum in PMIP2 simulations. Climate Dynamics 32, 525–548.

Russell, J.L., Dixon, K.W., Gnanadesikan, A., Stouffer, R.J., Toggweiler, J.R., 2006. The Southern Hemisphere westerlies in a warming world: propping open the door to the deep ocean. Journal of Climate 19, 6382–6390.

Sagredo, E.A., Moreno, P.I., Villa-Martínez, R., Kaplan, M.R., Kubik, P.W., Stern, C.R., 2011. Fluctuations of the Última Esperanza Ice Lobe (52°S), Chilean Patagonia, during the Last Glacial Maximum and Termination 1. Geomorphology. ISSN: 0169-555X 125 (1). ISSN: 0169-555X, 92–108. doi:10.1016/j.geomorph.2010.09.007.

Stern, C.R., 2008. Holocene tephrochronology record of large explosive eruptions in the southernmost Patagonian Andes. Bulletin of Volcanology 70, 435–454.

Stern, C.R., Moreno, P.I., Villa-Martínez, R., Sagredo, E.A., Prieto, A., Labarca, R., 2011. The late-glacial R1 eruption of Reclús volcano, Andean Austral Volcanic Zone: implications for evolution of ice-dammed proglacial lakes in Última Esperanza, Chile. Andean Geology 38, 82–97.

Strelin, J.A., Denton, G.H., Vandergoes, M.J., Ninnemann, U.S., Putnam, A.E., 2011. Radiocarbon Chronology of the Late-Glacial Puerto Bandera Moraines. Southern Patagonian Icefield, Argentina. doi:10.1016/j.quascirev.2011.05.004. Quaternary Science Reviews.

Sugden, D.E., Bentley, M.J., Fogwill, C.J., Hulton, N.R.J., McCulloch, R.D., Purves, R.S., 2005. Late-glacial glacier events in Southernmost South America: a blend of 'northern' and 'southern' Hemispheric climatic signals? Geografiska Annaler Series A 87, 273–288.

Toggweiler, J.R., 2009. Shifting Westerlies. Science 323, 1434–1435.

Toggweiler, J.R., Russell, J.L., Carson, S.R., 2006. Midlatitude westerlies, atmospheric CO_2, and climate change during the ice ages. Paleoceanography 21.

Toggweiler, J.R., Samuels, B., 1995. Effect of drake passage on the global thermohaline circulation. Deep-Sea Research Part I-Oceanographic Research Papers 42, 477–500.

Villa-Martínez, R., Moreno, P.I., 2007. Pollen evidence for variations in the southern margin of the westerly winds in SW Patagonia over the last 12,600 years. Quaternary Research 68, 400–409.

Villa-Martínez, R., Moreno, P.I., Valenzuela, M.A., 2012. Deglacial and postglacial vegetation changes on the eastern slopes of the central Patagonian Andes (47°S). Quaternary Science Reviews 32, 86–99.

Walker, M., Johnsen, S., Rasmussen, S.O., Popp, T., Steffensen, J.-P., Gibbard, P., Hoek, W., Lowe, J., Andrews, J., Björck, S., Cwynar, L.C., Hughen, K., Kershaw, P., Kromer, B., Litt, T., Lowe, D.J., Nakagawa, T., Newnham, R., Schwander, J., 2009. Formal definition and dating of the GSSP (Global Stratotype Section and Point) for the base of the Holocene using the Greenland NGRIP ice core, and selected auxiliary records. Journal of Quaternary Science 24, 3–17.

Whitlock, C., Anderson, R.S., 2003. Fire history reconstructions based on sediment records from lakes and wetlands. In: Veblen, T.T., Baker, W.L., Montenegro, G., Swetnam, T.W. (Eds.), Fire and Climatic Change in Temperate Ecosystems of the Western Americas. Springer, New York, pp. 265–295.

Whitlock, C., Moreno, P.I., Bartlein, P., 2007. Climatic controls of Holocene fire patterns in southern South America. Quaternary Research 68, 28–36.